Supplementary Information

Self-Assembly of Photochromic Diarylethene–Peptide Conjugates Stabilized by β-Sheet Formation at the Liquid/Graphite Interface

Nobuhiko Nishitani,[a] Takashi Hirose[b] and Kenji Matsuda*[a]

[a] *Department of Synthetic Chemistry and Biological Chemistry, Graduate School of Engineering, Kyoto University, Katsura, Nishikyo-ku, Kyoto 615-8510, Japan*

[b] *Institute for Chemical Research, Kyoto University, Uji, Kyoto 611-0011, Japan*

E-mail: kmatsuda@sbchem.kyoto-u.ac.jp

Contents:

Experimental Details

A. Synthesis of Materials S1
B. UV-vis. and CD Spectroscopies, and Photochemical Reactions S4
C. STM Measurement S5
D. Molecular Modeling S5

Supporting Data

Figure S1. UV-vis. absorption spectra of **1** in octanoic acid S6
Figure S2, S3 Concentration-dependent absorption spectra of **1o** and **2o** in octanoic acid. S6
Figure S4 CD spectra of **1o** and **2o** in octanoic acid. S7
Figure S5. STM images of **1** at the octanoic acid/HOPG interface S7
Table S1. Statistic data of concentration dependence of surface coverage for **2o** S8
Figure S6–S11. STM images of **2o** at different concentration conditions S8
Figure S12. Histograms of surface coverage of **2o** S10
Figure S13. Optimized molecular model of the 2-D ordering of **2o** using MM/MD calculations S11
Table S2, S3. Energy contributions of **2o** and **3o** on HOPG substrate with MM calculation S12
Table S3, S4. Adsorption energies of **2o** and **3o** in molecular orderings on HOPG Substrate S13
Figure S14–S29. ^{1}H and ^{13}C NMR spectra of compounds **4**, **5**, **7**–**10**, **1o**, and **2o** S14

References S22

Experimental Details

A. Synthesis of materials

General. Unless specifically mentioned, reagents and solvents were obtained from commercial suppliers and used without further purification. All reactions were monitored by thin-layer chromatography carried out on 0.2 mm Merck silica gel plates (60F-254). Column chromatography was performed on silica gel (Nacalai Tesque, 70–230 mesh for normal phase) or on a Biotage Instrument (Isolera One) with a SNAP flash silica gel cartridge (KP-Sil). Final products were purified by a preparative gel permeation chromatography (GPC) (Japan Analytical Industry Co., Ltd., JAIGEL-1H and 2H, eluent: chloroform). ^{1}H and ^{13}C NMR spectra were recorded on a JEOL JNM-ECS400, a JEOL JNM-ALPHA500, or a JNM-ECA600 instrument. Proton chemical shifts are reported in ppm downfield from tetramethylsilane (TMS). Mass spectra were obtained by a JEOL JMS-HX110A or a Thermo Fisher Scientific LTQ Orbitrap XL mass spectrometer. *N,N*-dimethylformamide (DMF) and dichloromethane were dried with calcium hydride and then distilled before use. Compound **6**[S1] has been prepared according to the literature procedure. Azeotropic mixture of formic acid/triethylamine (5/2) (triethylammonium formate, TEAF) was prepared as follows: triethylamine (16.2 g, 0.16 mol) was slowly added to a stirred formic acid (18.4 g, 0.40 mol) at 0 °C.[S2]

Scheme 1. Synthesis of Compound **1o**.

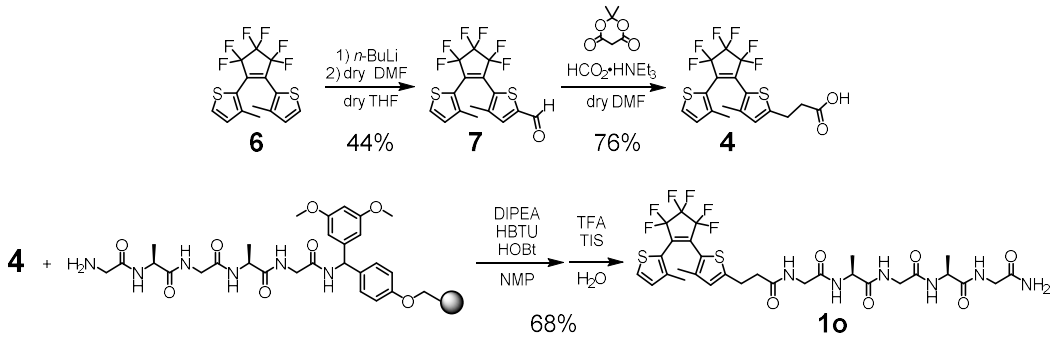

Synthesis of 1-(5-formyl-3-methyl-2-thienyl)-2-(3-methyl-2-thienyl)hexafluorocyclopentene (7)

To a solution of **6** (500 mg, 1.36 mmol) in dry ether (5 mL) was slowly added dropwise *n*-BuLi (1.6 M in hexane, 0.85 mL, 1.36 mmol) at 0 °C under nitrogen atmosphere. After the mixture was stirred for 30 min at that temperature, dry DMF (1.0 mL, 12.9 mmol) was added into the solution. The solution was allowed to warm to room temperature and stirred for 1 h. The reaction was quenched by the addition of water. The reaction product was extracted with hexane. The combined organic layers were washed with brine, dried over $MgSO_4$, filtrated, and evaporated. The crude product was purified by silica gel chromatography (hexane/CH_2Cl_2 = 1:1) to yield **7** (235 mg, 0.592 mmol, 44%) as a brown solid.

7: ^{1}H NMR (500 MHz, $CDCl_3$, δ): 1.82 (s, 3H), 1.83 (s, 3H), 6.87 (d, J = 5.0 Hz, 1H), 7.49 (d, J = 5.0 Hz, 1H), 7.51 (s, 1H), 9.87 (s, 1H); ^{13}C NMR (126 MHz, $CDCl_3$, δ): 14.9, 15.3, 108.5 (t), 110.7 (t), 113.0 (m), 115.3 (t), 117.3 (t), 112.3, 130.3, 131.0, 132.0, 133.0 (t), 137.8 (t), 138.0, 141.66, 141.73, 145.2, 182.5; HRMS–MALDI–orbitrap (*m*/*z*): $[M + H]^+$ calcd for $C_{16}H_{11}F_6OS_2^+$, 397.0150; found, 397.0140.

*Synthesis of 1-(5-(2-carboxyethyl)-3-methyl-2-thienyl)-2-(3-methyl-2-thienyl)hexafluorocyclopentene (**4**)*

To a solution of **7** (480 mg, 1.21 mmol) in dry DMF (8 mL) and TEAF (8 mL) was added Meldrum's acid (180 mg, 1.25 mmol). The solution was stirred for 4 h at room temperature. The solution was stirred for 4h at 100 °C. The resulting solution was then cooled to room temperature and cooled water (10 g) was added. The solution was acidified with concentrated aq. HCl until pH became 1. The reaction product was extracted with ether. Combined organic layers were then extracted with aq. NaOH (1 N) and the aqueous layer was washed with ether. The aqueous layer was neutralized with concentrated aq. HCl, and the reaction product was extracted with ether. The combined organic layers were washed with brine, dried over Na_2SO_4, filtrated, and evaporated. The crude product was purified by reversed phase chromatography (MeOH/H_2O = 8:2) to yield **4** (405 mg, 0.920 mmol, 76%) as a pale yellow solid.
4: ^{1}H NMR (400 MHz, $CDCl_3$, δ): 1.68 (s, 3H), 1.77 (s, 3H), 2.72 (t, *J* = 7.6 Hz, 2H), 3.10 (t, *J* = 7.2 Hz, 2H), 6.58 (s, 1H), 6.83 (d, *J* = 5.2 Hz, 1H), 7.43 (d, *J* = 4.8 Hz, 1H); ^{13}C NMR (101 MHz, $CDCl_3$, δ): 15.0, 15.1, 24.9, 35.4, 108.1 (q), 110.8 (q), 113.1 (t), 113.5 (q), 115.6 (t), 118.2 (t), 121.5, 123.1, 128.7, 129.3, 130.6, 134.0 (t), 134.6 (t), 141.0, 141.3, 178.4; HRMS–ESI–orbitrap (*m*/*z*): $[M - H]^+$ calcd for $C_{18}H_{13}F_6O_2S_2^+$, 439.0256; found, 439.0260.

*Synthesis of **1o***

The solid-phase synthesis was carried out using Rink Amide resin (Novabiochem) (425 mg, 0.47 mmol/g initial loading). Fmoc-Ala-OH and Fmoc-Gly-OH were used as building blocks. Fmoc deprotection was performed with 20% piperidine in N-methylpyrrolidone (NMP). Amino acid coupling reactions were performed with a mixture of Fmoc-amino acid (3 eq), HBTU (3 eq), HOBt (3 eq), and DIPEA (6 eq) in NMP. The coupling of **1o** was performed with a mixture of **4** (1.5 eq), HBTU (1.5 eq), HOBt (1.5 eq), and DIPEA (3 eq) in NMP. All coupling and Fmoc deprotection steps were monitored by the Kaiser test. Following assembly, global deprotection and cleavage from the resin was performed with TFA containing 2.5% TIS and 2.5% H_2O. The crude peptide products were purified by reprecipitation with iced ether from MeOH to yield **1o** (102 mg, 0.136 mmol, 68%) as a pale yellow solid.
1o: ^{1}H NMR (400 MHz, CD_3OD/D_2O = 9:1, δ): 1.39 (d, *J* = 7.2 Hz, 3H), 1.40 (d, *J* = 7.2 Hz, 3H), 1.65 (s, 3H), 1.75 (s, 3H), 2.63 (t, *J* = 7.5 Hz, 2H), 3.11 (t, *J* = 7.5 Hz, 2H), 3.8–4.0 (m, 6H), 4.30 (quart, *J* = 7.2 Hz, 2H), 6.72 (s, 1H), 6.95 (d, *J* = 5.1 Hz, 1H), 7.66 (d, *J* = 5.1 Hz, 1H); ^{13}C NMR (151 MHz, CD_3OD/D_2O = 9:1, δ): 15.26, 15.35, 17.39, 17.41, 26.6, 38.0, 43.3, 43.6, 43.8, 51.11, 51.15, 108.0–113.0 (m), 114.0–119.0 (m), 121.9, 123.9, 130.1, 131.1, 131.9, 135.3 (m), 135.9 (m), 142.7, 143.0, 149.9, 172.0, 172.2, 174.6, 175.0, 175.5, 176.1; HRMS–MALDI–orbitrap (*m*/*z*): $[M + Na]^+$ calcd for $C_{30}H_{34}F_6N_6O_6S_2Na^+$, 775.1778; found, 775.1792.

Scheme 2. Synthesis of Compound **2o**.

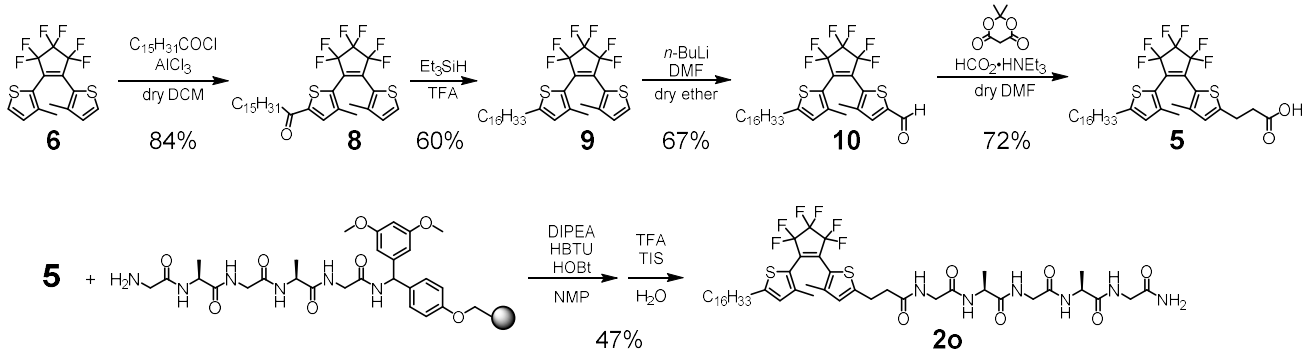

*Synthesis of 1-(5-hexadecanoyl-3-methyl-2-thienyl)-2-(3-methyl-2-thienyl)hexafluorocyclopentene (**8**)*

To a solution of **6** (800 mg, 2.17 mmol) and $C_{15}H_{31}COCl$ (0.72 mL, 2.38 mmol) in dry CH_2Cl_2 (20 mL) was added $AlCl_3$ (440 mg, 3.30 mmol) at 0 °C. The solution was stirred for 2 h at 0 °C. The solution was allowed to warm to room temperature and stirred for 4 h. The reaction mixture was poured into ice water, then the reaction product was extracted with CH_2Cl_2. The combined organic layers were washed with brine, dried over $MgSO_4$, filtrated, and evaporated. The crude product was purified by silica gel chromatography (hexane/CH_2Cl_2 = 8:2) to yield **8** (1.11 g, 1.81 mmol, 84%) as an orange oil.

8: ^{1}H NMR (400 MHz, $CDCl_3$, δ): 0.88 (t, *J* = 7.2 Hz, 3H), 1.21–1.39 (m, 24H), 1.69–1.88 (m, 8H), 2.81–2.88 (m, 2H), 6.81–6.86 (m, 1H), 7.38–7.48 (m, 2H); ^{13}C NMR (101 MHz, $CDCl_3$, δ): 14.1, 15.1, 15.3, 22.7, 24.5, 29.26, 29.36, 29.38, 29.5, 29.60, 29.65, 29.67, 31.9, 39.4, 129.4–131.0 (m), 133.4, 133.9, 141.5, 145.5, 145.9, 193.0; HRMS–MALDI–orbitrap (*m*/*z*): $[M + H]^+$ calcd for $C_{31}H_{41}F_6OS_2^+$, 607.2498; found, 607.2476.

*Synthesis of 1-(5-hexadecyl-3-methyl-2-thienyl)-2-(3-methyl-2-thienyl)hexafluorocyclopentene (**9**)*

To a solution of **9** (500 mg, 0.824 mmol) in TFA (5 mL) was added dropwise Et_3SiH (0.55 mL, 3.44 mmol). The solution was stirred for 10 h at room temperature. The reaction product was extracted with CH_2Cl_2. The combined organic layers were washed with aq. $NaHCO_3$ and brine, dried over $MgSO_4$, filtrated, and evaporated. The crude product was purified by silica gel chromatography (hexane) to yield **9** (293 mg, 0.494 mmol, 60%) as a yellow solid.

9: ^{1}H NMR (400 MHz, $CDCl_3$, δ): 0.88 (t, *J* = 7.2 Hz, 3H), 1.21–1.31 (m, 26H), 1.54–1.82 (m, 8H), 2.74 (t, *J* = 7.7 Hz, 2H), 6.49–6.51 (m, 1H), 6.81–6.84 (m, 1H), 7.39–7.43 (m, 1H); ^{13}C NMR (101 MHz, $CDCl_3$, δ): 14.1, 15.0, 15.2, 22.7, 29.0, 29.3, 29.4, 29.51, 29.59, 29.65, 29.69, 30.0, 31.3, 31.9, 120.4, 128.0, 129.0, 130.5, 140.8, 141.2, 150.5; HRMS–MALDI–orbitrap (*m*/*z*): $[M]^+$ calcd for $C_{31}H_{42}F_6S_2^+$, 592.2627; found, 593.2618.

*Synthesis of 1-(5-formyl-3-methyl-2-thienyl)-2-(5-hexadecyl-3-methyl-2-thienyl)hexafluorocyclopentene (**10**)*

To a solution of **9** (100 mg, 0.169 mmol) in dry ether (5 mL) was slowly added dropwise *n*-BuLi (1.6 M in hexane, 120 μL, 0.192 mmol) at 0 °C under N_2 atmosphere. After the mixture was stirred for 30 min at that temperature, dry DMF (1.0 mL, 12.9 mmol) was added into the solution. The solution was allowed to warm to room temperature and stirred for 1 h. The reaction was quenched by the addition of water. The reaction product was extracted with hexane. The combined organic layers were washed with brine, dried over $MgSO_4$, filtrated, and evaporated. The crude product was purified by silica gel chromatography (hexane/CH_2Cl_2 = 7:3) to yield **10** (70.0 mg, 0.113 mmol, 67%) as a yellow solid.

10: ^{1}H NMR (600 MHz, $CDCl_3$, δ): 0.88 (t, *J* = 6.9 Hz, 3H), 1.23–1.31 (m, 26H), 1.64 (quint, *J* = 7.8 Hz), 1.74 (s, 3H), 1.82 (s, 3H), 2.74 (t, *J* = 7.6 Hz, 2H), 6.55 (s, 1H), 7.51 (s, 1H), 9.87 (s, 1H); ^{13}C NMR (151 MHz, $CDCl_3$, δ): 14.1, 15.0, 15.5, 22.7, 29.0, 29.2, 29.3, 29.5, 29.60, 29.64, 29.7, 30.1, 31.2, 31.9, 108.7–112.6 (m), 113.5–117.3 (m), 119.8, 128.5, 131.2 (t), 137.7–137.9 (m), 138.0, 141.5, 142.0, 145.0, 151.8 182.5; HRMS–MALDI–orbitrap (*m*/*z*): $[M + H]^+$ calcd for $C_{32}H_{43}F_6OS_2^+$, 621.2654; found, 621.2629.

*Synthesis of 1-(5-(2-carboxyethyl)-3-methyl-2-thienyl)-2-(5-hexadecyl-3-methyl-2-thienyl)hexafluorocyclopentene (**5**)*

To a solution of **10** (70.0 mg, 0.113 mmol) in dry DMF (3 mL) and TEAF (3 mL) was added Meldrum's acid (18.0 mg, 0.124 mmol). The solution was stirred for 8h at 100 °C. The resulting solution was then cooled to room temperature and cooled water (10 g) was added. The solution was acidified with concentrated aq. HCl until pH became 1. The reaction product was extracted with ether. The combined organic layers were washed with brine, dried over Na_2SO_4, filtrated, and evaporated. The crude product was purified by reversed phase chromatography (acetone/H_2O = 9:1) to yield **5** (53.8 mg, 0.0809 mmol, 72%) as a yellow solid.

5: ^{1}H NMR (400 MHz, $CDCl_3$, δ): 0.88 (t, *J* = 7.2 Hz, 3H), 1.24–1.40 (m, 26H), 1.59–1.69 (m, 8H), 2.73 (q, J = 7.6 Hz, 4H), 3.10 (t, J = 7.4 Hz, 2H), 6.51 (s, 1H), 6.58 (s, 1H); ^{13}C NMR (101 MHz, $CDCl_3$, δ): 14.1, 15.1, 15.2, 22.7, 25.0, 29.0, 29.3, 29.4, 29.5, 29.62, 29.66, 29.70, 30.1, 31.3, 31.9, 35.4, 108.4–118.3 (m), 120.6, 121.6, 133.3–134.6 (m), 141.06, 141.11, 146.7, 150.5, 178.0. HRMS–MALDI–orbitrap (*m*/*z*): $[M]^+$ calcd for $C_{34}H_{46}F_6O_2S_2^+$, 664.2838; found, 664.2825.

*Synthesis of **2o***

Compound **2o** was prepared by Fmoc solid-phase peptide synthesis on a Biotage Initiator+ microwave peptide synthesizer. The synthesis was carried out using Rink Amide resin (Novabiochem) (115 mg, 0.47 mmol/g initial loading) in a 10 mL reactor vial. Fmoc-Ala-OH and Fmoc-Gly-OH were used as building blocks. Fmoc deprotection was performed with 20% piperidine in N-methylpyrrolidone (NMP). Amino acid coupling reactions were performed with a mixture of Fmoc-amino acid (3 eq), HBTU (3 eq), HOBt (3 eq), and DIPEA (6 eq) in NMP. The coupling of **2o** was performed with a mixture of **5** (1.5 eq), HBTU (1.5 eq), HOBt (1.5 eq), and DIPEA (3 eq) in NMP. A coupling time of 10 minutes at 75 °C was employed. All coupling and Fmoc deprotection steps were monitored by the Kaiser test. Following assembly, global deprotection and cleavage from the resin was performed with TFA containing 2.5% TIS and 2.5% H_2O. The crude peptide products were purified by reprecipitation with iced ether from $CHCl_3$/MeOH (7:3) to yield **2o** (25 mg, 0.0256 mmol, 47%) as a pale yellow solid.

2o: ^{1}H NMR (500 MHz, $CDCl_3$/CD_3OD = 7:3, δ): 0.88 (t, *J* = 6.0 Hz, 3H), 1.23–1.35 (m, 28H), 1.38–1.42 (m, 6H), 1.67 (s, 6H), 2.61 (t, *J* = 7.5 Hz, 2H), 2.77 (t, *J* = 8.0 Hz, 2H), 3.09–3.12 (m, 2H), 3.76–3.95 (m, 6H), 4.23–4.34 (m, 2H), 6.55 (s, 1H), 6.61 (s, 1H); ^{13}C NMR (151 MHz, $CDCl_3$/CD_3OD = 7:3, δ): 14.2, 15.2, 15.3, 16.9, 22.9, 25.9, 29.3, 29.5, 29.6, 29.77, 29.86, 29.91, 29.94, 30.3, 31.6, 32.2, 37.2, 42.7, 43.1, 43.4, 50.1, 50.3, 120.8, 121.6, 128.3, 128.9, 141.5, 147.8, 150.9, 170.9, 171.0, 173.3, 173.7, 174.0, 174.8; HRMS–MALDI–orbitrap (*m*/*z*): $[M + Na]^+$ calcd for $C_{46}H_{66}F_6N_6O_6S_2Na^+$, 999.4282; found, 999.4277.

B. UV-vis. and CD Spectroscopies, and Photochemical Reactions

UV-vis. absorption spectra were measured on a JASCO V-670 spectrophotometer equipped with a ETCS-761 Peltier-type temperature controller. CD spectra were measured on a JASCO J-720WI (conditions: scan rate, 200 nm/min; response, 0.5 sec; band width, 2.0 nm) equipped with a PIC-348WI Peltier-type temperature controller. A quartz cuvette with 2, 5, and 10 mm optical path was used for the spectroscopic measurements. Photochemical reactions in an optical cell were performed using a USHIO super-high-pressure mercury lamp (500 W). Mercury line

of 313 nm was isolated by passing the light though a combination of a sharp-cut filter (UV-29) and a monochrometer (Ritu Oyo Kougaku Co., Ltd. MC-20L). For the STM measurement in Figure 5, UV light (313 nm) was irradiated for 30 min before the deposition on HOPG substrate to prepare a solution containing the closed-ring isomer **2c** (c_t = 200 μM). The conversion ratio of the solution was precisely determined using UV-vis absorption measurement at **2o**/**2c** = 60/40, which was used for STM measurements.

C. STM Measurement

All STM experiments were performed at room temperature and ambient conditions. The STM images were acquired with an Agilent technologies 5500 scanning probe microscopes in the constant current mode. The STM tips used in this research were mechanically cut from a Pt/Ir wire (80/20, diameter 0.25 mm). Highly oriented pyrolytic graphite (HOPG) (purchased from the Bruker Co.) was used as a substrate. Homogeneous solutions of **1o** and **2o** in octanoic acid were prepared by heating solution or under ultrasonic wave before STM measurements. A drop of the solution (8 μL) was deposited onto a freshly cleaved HOPG surface, and the tip was immersed into the solution and then the image was scanned. Lattice constants of molecular orderings were determined based on the high-resolution STM images using the graphite substrate as a calibration grid. Surface coverage of each STM image was defined as the fraction of surface area where molecular ordering was observed. The total STM scans were performed 15 times in order to determine an averaged surface coverage at each concentration of sample solution.

D. Molecular Modeling

The molecular ordering adsorbed on HOPG surface was modeled by a molecular mechanics/molecular dynamics (MM/MD) approach using Materials Studio 2018, Accelrys Software Inc. The Dreiding force field implemented in the Forcite module was used for MM and MD calculations. The initial geometries were inspired from experimentally observed high resolution STM images for each ordering. For HOPG substrate, only one layer of graphene sheet (C-C bond length is 1.42 Å, flat geometry having hexagonal symmetry) was assumed. The Cartesian position of the graphene sheet was fixed during MM/MD calculations to suppress deformation/distortion of substrate.

Supporting Data

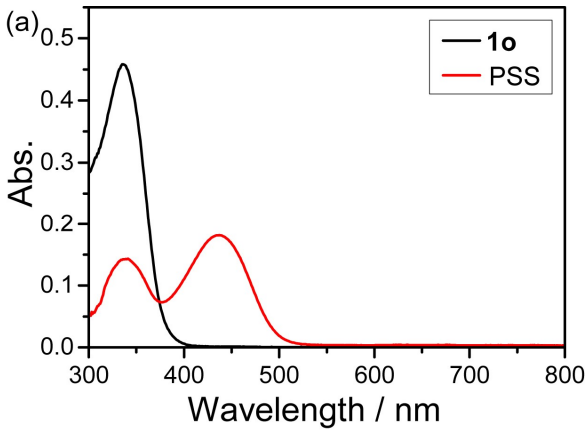

Figure S1. UV-vis. spectral change of **1** in octanoic acid upon photoisomerization (c = 40 μM, cell length: 10 mm).

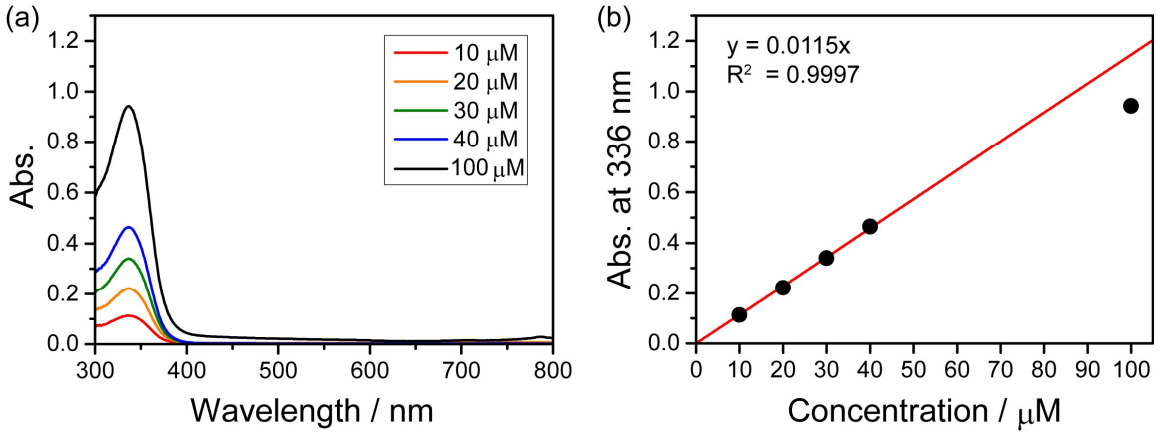

Figure S2. (a) UV-vis absorption spectra of **1o** in octanoic acid (cell length: 10 mm). (b) The plot of absorbance at 336 nm over concentration of **1o** in octanoic acid. The molar extinction coefficient (ε) of **1o** ($\varepsilon = 1.15 \times 10^4$ $M^{-1}cm^{-1}$ at 336 nm) was calculated from the slopes of the fitted line (red solid line).

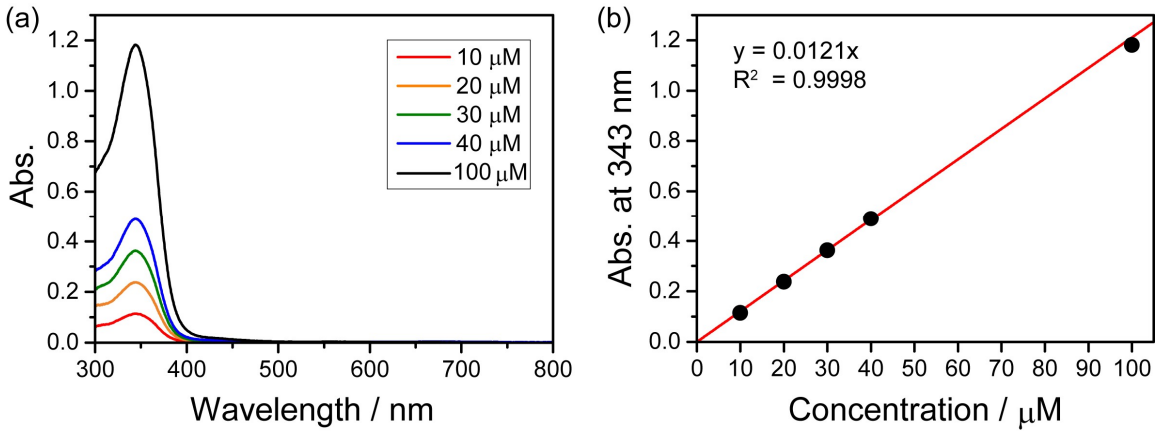

Figure S3. (a) UV-vis absorption spectra of **2o** in octanoic acid (cell length: 10 mm). (b) The plot of absorbance at 343 nm over concentration of **2o** in octanoic acid. The molar extinction coefficient (ε) of **2o** ($\varepsilon = 1.21 \times 10^4$ $M^{-1}cm^{-1}$ at 343 nm) was calculated from the slopes of the fitted line (red solid line).

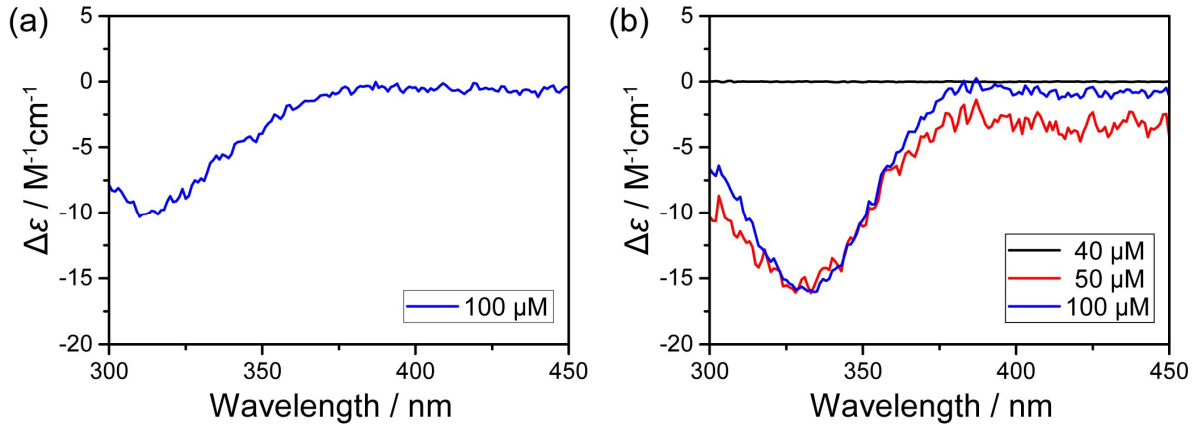

Figure S4. (a) CD spectra of **1o** in octanoic acid (c = 100 μM, cell length: 2 mm). (b) CD spectra of **2o** in octanoic acid (c = 40, 50, and 100 μM, cell length: 2 mm).

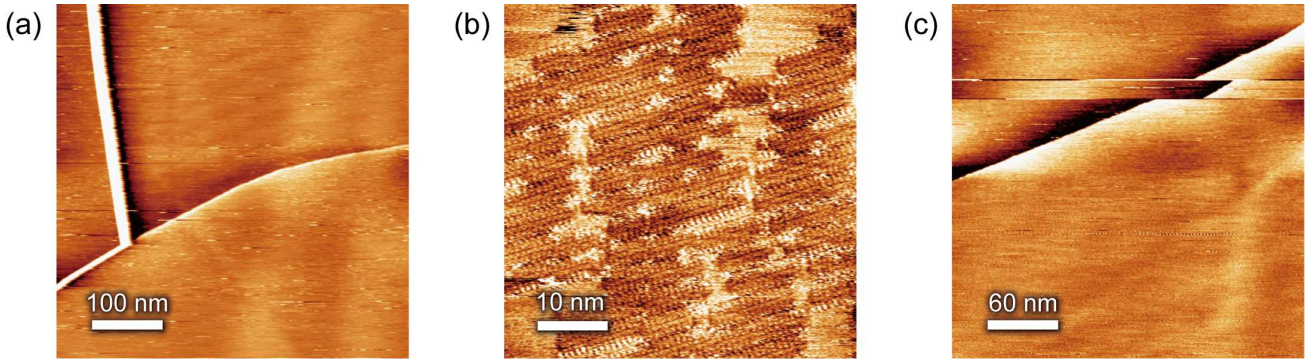

Figure S5. STM images of (a) **1o** at 200 μM, (b) **1o** in saturated solution, (c) **1PSS** in saturated solution at the octanoic acid/HOPG interface (I_{set} = 10 pA, V_{bias} = −800 – −1000 mV). We did not determine the unit cell for the 2-D ordering of **1o** due to poor reproducibility of the STM observation. In the STM image shown in Figure S5b, the lamella structure covered only small area on the HOPG surface less than 0.04 μm^2 even though a saturated solution of **1o** was used, and the structure tended to disappear during STM scans. For this reason, it was difficult to determine a reliable unit cell parameters for the ordering of **1o**.

Table S1. The list of surface coverage of **2o**.

/ μM	30	40	50	60	70	100
1	0	0	0	0	1	1
2	0	0	0	0	0.97	1
3	0	0	0	0	0.92	1
4	0	0	0.01	0	0.94	1
5	0	0	0	0	0.97	1
6	0	0	0.01	0.95	0.70	1
7	0	0	0.16	0.93	1	1
8	0	0	0.21	1	1	1
9	0	0	0.33	1	1	1
10	0	0	0.25	0.98	1	1
11	0	0	0.22	0.86	1	1
12	0	0	0.36	0.01	1	1
13	0	0	0	0.88	1	1
14	0	0	0	0.06	1	1
15	0	0	0	0	1	1
Average	0.00	0.00	0.10	0.44	0.97	1.00
Deviation	0.00	0.00	0.14	0.48	0.08	0.00

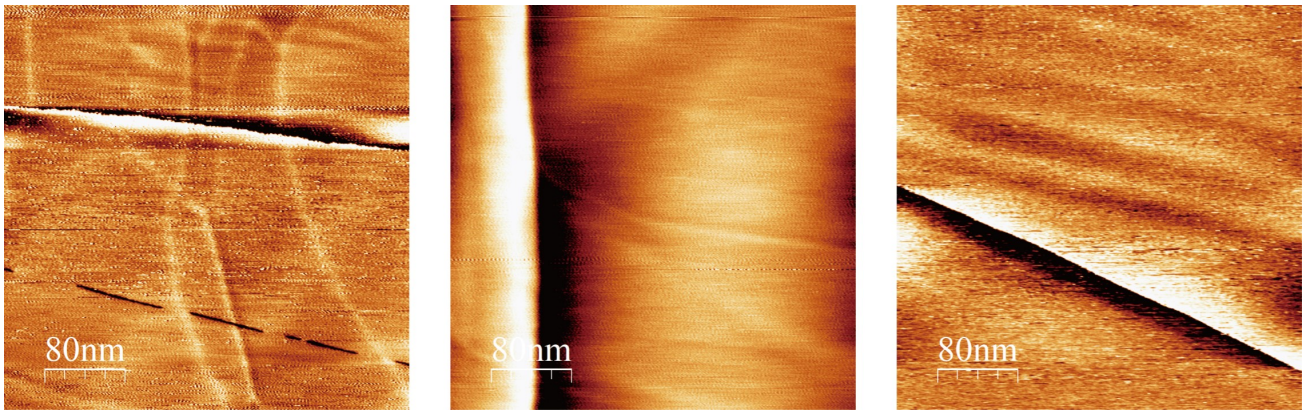

Figure S6. Representative STM images of the ordering of **2o** at 30 μM.

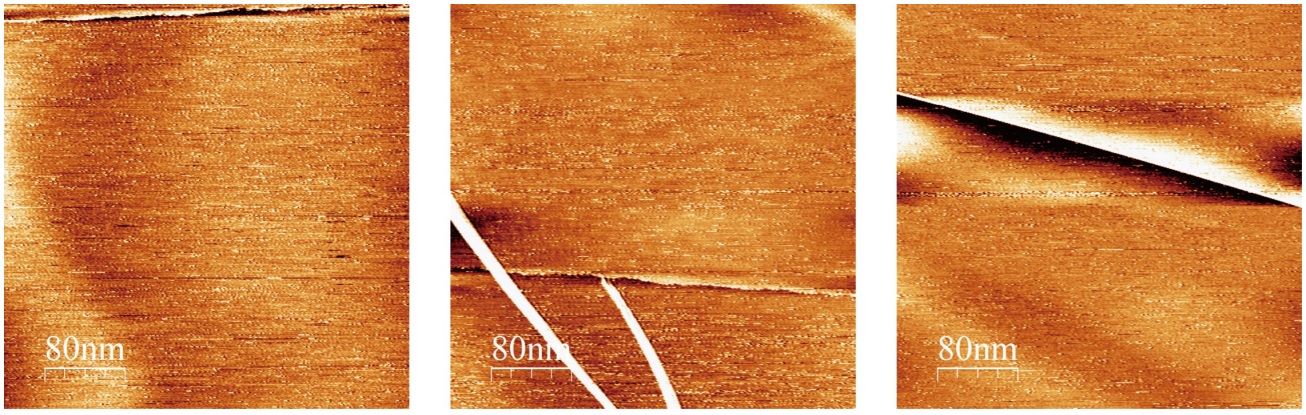

Figure S7. Representative STM images of the ordering of **2o** at 40 μM.

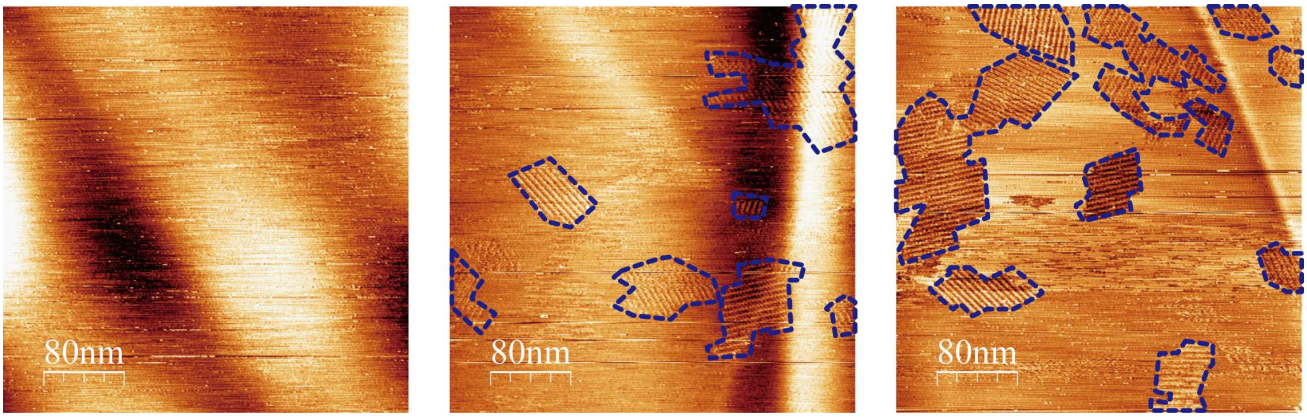

Figure S8. Representative STM images of the ordering of **2o** at 50 μM.

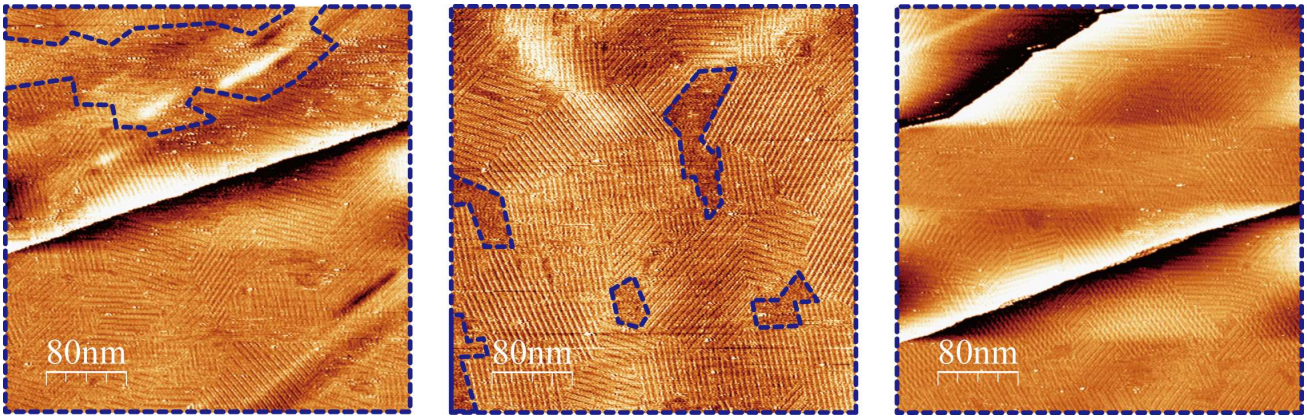

Figure S9. Representative STM images of the ordering of **2o** at 60 μM.

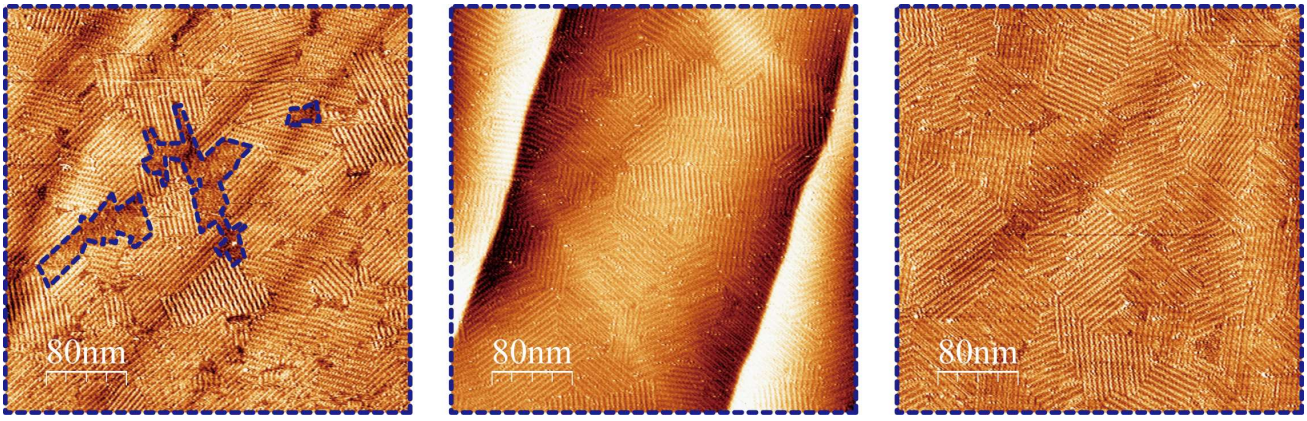

Figure S10. Representative STM images of the ordering of **2o** at 70 μM.

Figure S11. Representative STM images of the ordering of **2o** at 100 μM.

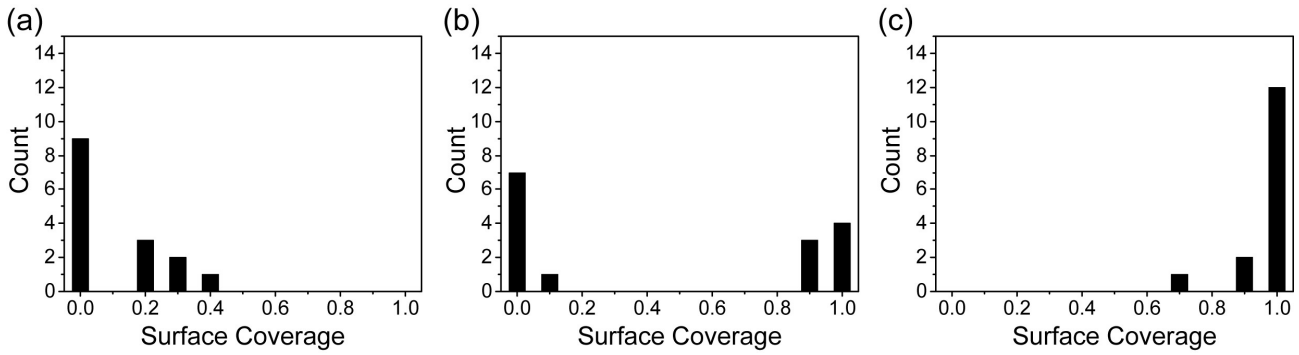

Figure S12. Histograms of surface coverage of **2o** at the octanoic acid/HOPG interface at concentrations of (a) 50, (b) 60, and (c) 70 μM. To obtain the histograms, 15 STM images were collected for each concentration. The typical scanning area of a STM image was 400 × 400 nm^2.

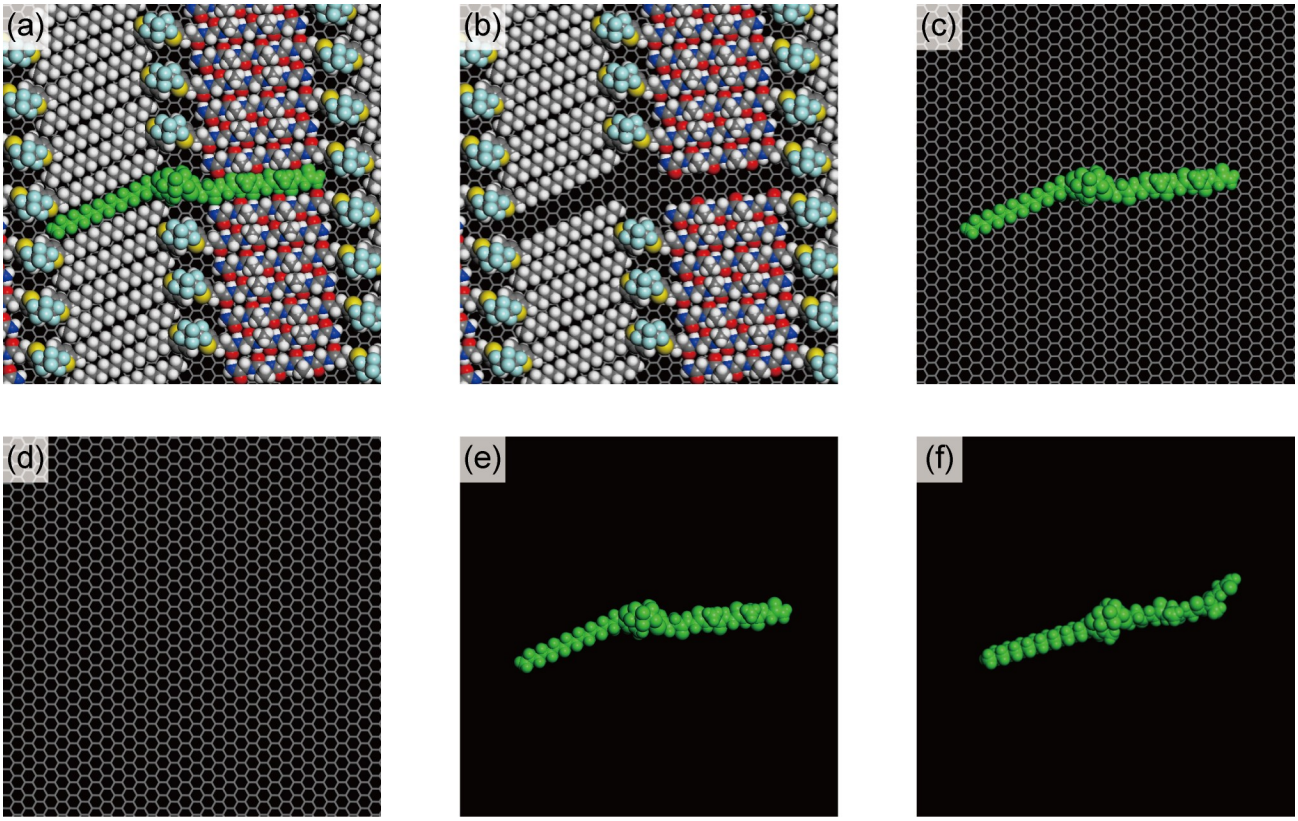

Figure S13. (a) Optimized molecular model of the 2-D ordering of **2o** composed of 48 molecules on HOPG substrate using MM/MD calculations (force field, Dreiding; quality, ultrafine). The total energy of the structure was $E_{\mathbf{2o}\_\text{ordering+HOPG}}$ = 372720.5 kJ·mol^{-1}. Molecular models for the single-point energy calculations: (b) one molecule of **2o** highlighted by green was removed from the 2-D ordering on HOPG ($E_{\mathbf{2o}\_\text{defect+HOPG}}$), (c) one molecule on HOPG ($E_{\mathbf{2o}\_\text{monomer+HOPG}}$), (d) HOPG substrate only (E_{HOPG}), (e) one molecule without HOPG ($E_{\mathbf{2o}(\text{surface})}$), and (f) **2o** optimized in gas phase without HOPG ($E_{\mathbf{2o}(\text{opted})}$). For the calculation of **3o**, optimized molecular model of the 2-D ordering of **3o** composed of 32 molecules on HOPG substrate reported in ref 40 were used. The total energy of each structure and energy contributions are summarized in Tables S2 and S3. It is noted that the effect of entropy change and interaction with solvent molecules were not taken into account in the calculation.

Table S2. Total energy and each energy contribution of a molecule of **2o** on HOPG substrate.[a]

	$E_{\mathbf{2o}\_\text{ordering+HOPG}}$[b] /kJ·mol^{-1}	$E_{\mathbf{2o}\_\text{defect+HOPG}}$[c] /kJ·mol^{-1}	$E_{\mathbf{2o}\_\text{monomer+HOPG}}$[d] /kJ·mol^{-1}	E_{HOPG}[e] /kJ·mol^{-1}	$E_{\mathbf{2o}(\text{surface})}$[f] /kJ·mol^{-1}	$E_{\mathbf{2o}(\text{opted})}$[g] /kJ·mol^{-1}
Total energy	372720.5	372839.8	371213.1	371054.2	535.1	463.2
Contributions to total energy						
Valence energy (diagonal terms)						
Bond	80598.7	80563.5	78969.4	78934.2	35.2	32.5
Angle	10241.8	10101.0	3770.3	3629.4	140.9	118.9
Torsion	5779.0	5659.3	119.7	0.0	119.7	96.7
Inversion	212.7	208.3	4.4	0.0	4.4	0.6
Non-bond energy						
Hydrogen bond	−2599.0	−2482.1	0.0	0.0	0.0	0.0
van der Waals	278487.2	278789.8	288349.2	288490.5	235.0	214.4

[a]Calculated with Forcite module implemented in Materials Studio 2018 in gas phase (force field, Dreiding; quality: ultra-fine). [b]Single-point energy of the molecular ordering of **2o** with HOPG substrate. [c]Single-point energy of the molecular model in which one molecule of **2o** was removed from the ordering on HOPG. [d]Single-point energy of one molecule of **2o** on HOPG. [e]Single-point energy of HOPG substrate. [f]Single-point energy of one molecule of **2o** without HOPG. [g]Energy of one molecule of **2o** optimized in gas phase without HOPG.

Table S3. Total energy and each energy contribution of a molecule of **3o** on HOPG substrate.[a]

	$E_{\mathbf{3o}\_\text{ordering+HOPG}}$[b] /kJ·mol^{-1}	$E_{\mathbf{3o}\_\text{defect+HOPG}}$[c] /kJ·mol^{-1}	$E_{\mathbf{3o}\_\text{monomer+HOPG}}$[d] /kJ·mol^{-1}	E_{HOPG}[e] /kJ·mol^{-1}	$E_{\mathbf{3o}(\text{surface})}$[f] /kJ·mol^{-1}	$E_{\mathbf{3o}(\text{opted})}$[g] /kJ·mol^{-1}
Total energy	174521.2	174636.6	175258.8	175217.3	426.3	413.7
Contributions to total energy						
Valence energy (diagonal terms)						
Bond	35194.5	35163.4	34221.4	34190.4	31.0	32.5
Angle	3803.4	3685.7	118.2	0.5	117.7	113.9
Torsion	3201.7	3101.8	99.9	0.0	99.9	97.0
Inversion	60.7	58.6	2.1	0.0	2.1	2.1
Non-bond energy						
Hydrogen bond	−612.0	−581.3	−10.5	0.0	−10.5	−10.3
van der Waals	132873.0	133208.4	140827.8	141026.5	186.2	178.6

[a]Calculated with Forcite module implemented in Materials Studio 2018 in gas phase (force field, Dreiding; quality: ultra-fine). [b]Single-point energy of the molecular ordering of **3o** with HOPG substrate. [c]Single-point energy of the molecular model in which one molecule of **3o** was removed from the ordering on HOPG. [d]Single-point energy of one molecule of **3o** on HOPG. [e]Single-point energy of HOPG substrate. [f]Single-point energy of one molecule of **3o** without HOPG. [g]Energy of one molecule of **3o** optimized in gas phase without HOPG.

Table S4. Adsorption energies of **2o** in molecular orderings on HOPG substrate[a]

	$E_{mol–sub}$ /kJ·mol^{-1} [b]	$E_{mol–mol}$ /kJ·mol^{-1} [c]	E_{strain} /kJ·mol^{-1} [d]
Total energy	−376.3	−139.1	72.0
Contributions to total energy			
Valence energy (diagonal terms)			
Bond	0.0	0.0	2.6
Angle	0.0	0.0	21.9
Torsion	0.0	0.0	23.0
Inversion	0.0	0.0	3.8
Non-bond energy			
Hydrogen bond	0.0	−58.4	0.0
van der Waals	−376.3	−80.6	20.6

[a]Calculated from total energy and each energy contribution of a molecule of **2o** on HOPG substrate summarized in Table S2. [b]The molecule–substrate interaction energy calculated as follows, $E_{mol–sub} = E_{\mathbf{2o}+HOPG} - (E_{\mathbf{2o}(surface)} + E_{HOPG})$. [c]The molecule–molecule interaction energy calculated as follows, $E_{mol–mol} = \{E_{\mathbf{2o}\_ordering+HOPG} - (E_{\mathbf{2o}\_defect+HOPG} + E_{\mathbf{2o}(surface)}) - E_{mol–sub}\}/2$. [d]The strain energy for the extended flat conformation on HOPG substrate calculated as follows, $E_{strain} = E_{\mathbf{2o}(surface)} - E_{\mathbf{2o}(opted)}$. Other contributions such as (1) effects of entropy and (2) solvent interactions were not taken into account in this calculation.

Table S5. Adsorption energies of **3o** in molecular orderings on HOPG substrate[a]

	$E_{mol–sub}$ /kJ·mol^{-1} [b]	$E_{mol–mol}$ /kJ·mol^{-1} [c]	E_{strain} /kJ·mol^{-1} [d]
Total energy	−384.8	−78.4	12.6
Contributions to total energy			
Valence energy (diagonal terms)			
Bond	0.0	0.0	−1.4
Angle	0.0	0.0	3.8
Torsion	0.0	0.0	2.8
Inversion	0.0	0.0	0.0
Non-bond energy			
Hydrogen bond	0.0	−10.1	−0.2
van der Waals	−384.8	−68.4	7.6

[a]Calculated from total energy and each energy contribution of a molecule of **3o** on HOPG substrate summarized in Table S3. [b]The molecule–substrate interaction energy calculated as follows, $E_{mol–sub} = E_{\mathbf{3o}+HOPG} - (E_{\mathbf{3o}(surface)} + E_{HOPG})$. [c]The molecule–molecule interaction energy calculated as follows, $E_{mol–mol} = \{E_{\mathbf{3o}\_ordering+HOPG} - (E_{\mathbf{3o}\_defect+HOPG} + E_{\mathbf{3o}(surface)}) - E_{mol–sub}\}/2$. [d]The strain energy for the extended flat conformation on HOPG substrate calculated as follows, $E_{strain} = E_{\mathbf{3o}(surface)} - E_{\mathbf{3o}(opted)}$. Other contributions such as (1) effects of entropy and (2) solvent interactions were not taken into account in this calculation.

^{1}H and ^{13}C NMR spectra of compounds **4**, **5**, **7**–**10**, **1o**, and **2o**

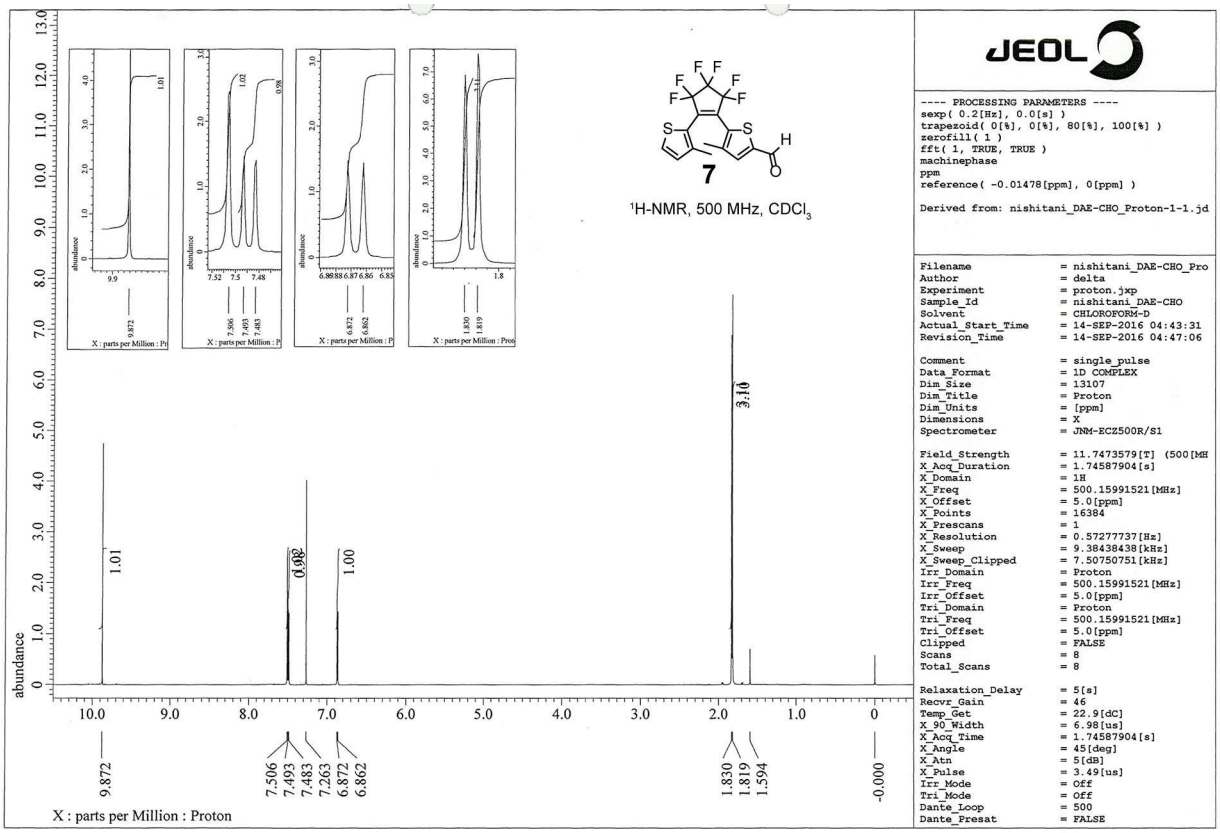

Figure S14. ^{1}H NMR spectra of compound **7** ($CDCl_3$, 500 MHz)

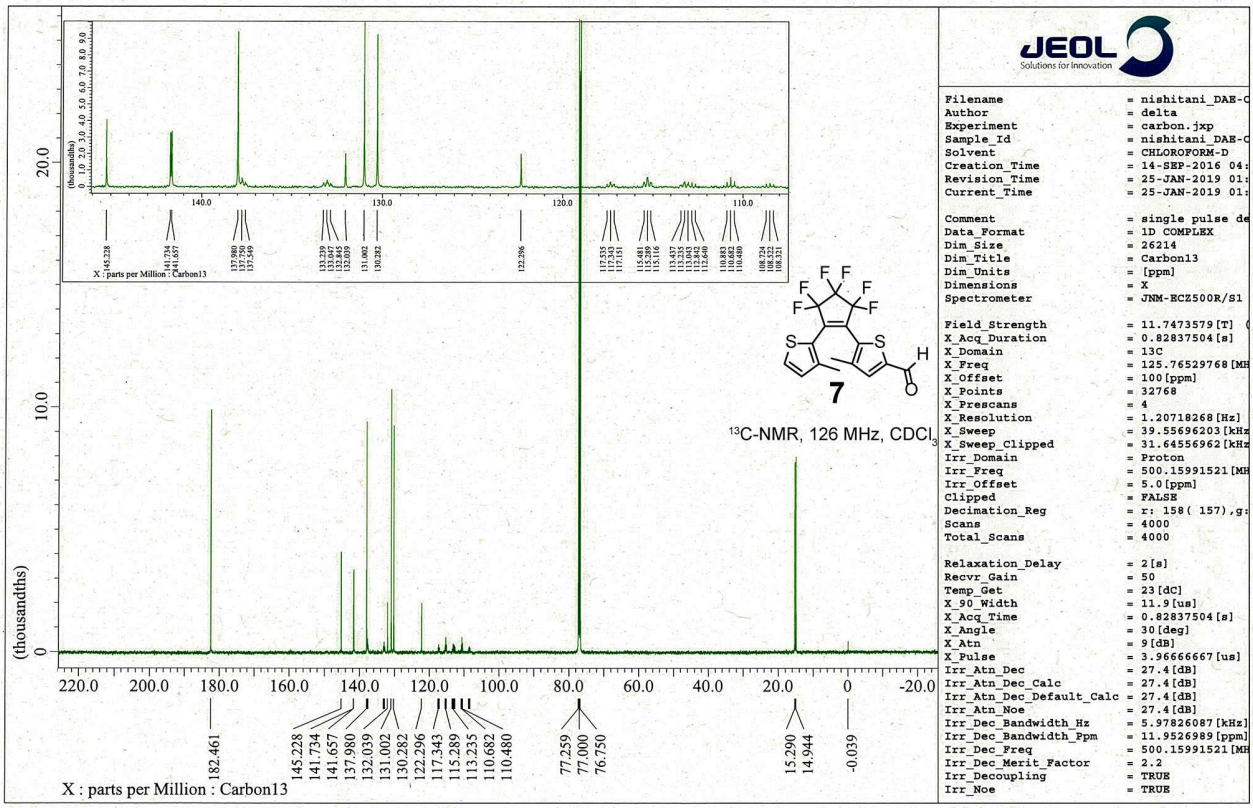

Figure S15. ^{13}C NMR spectra of compound **7** ($CDCl_3$, 126 MHz)

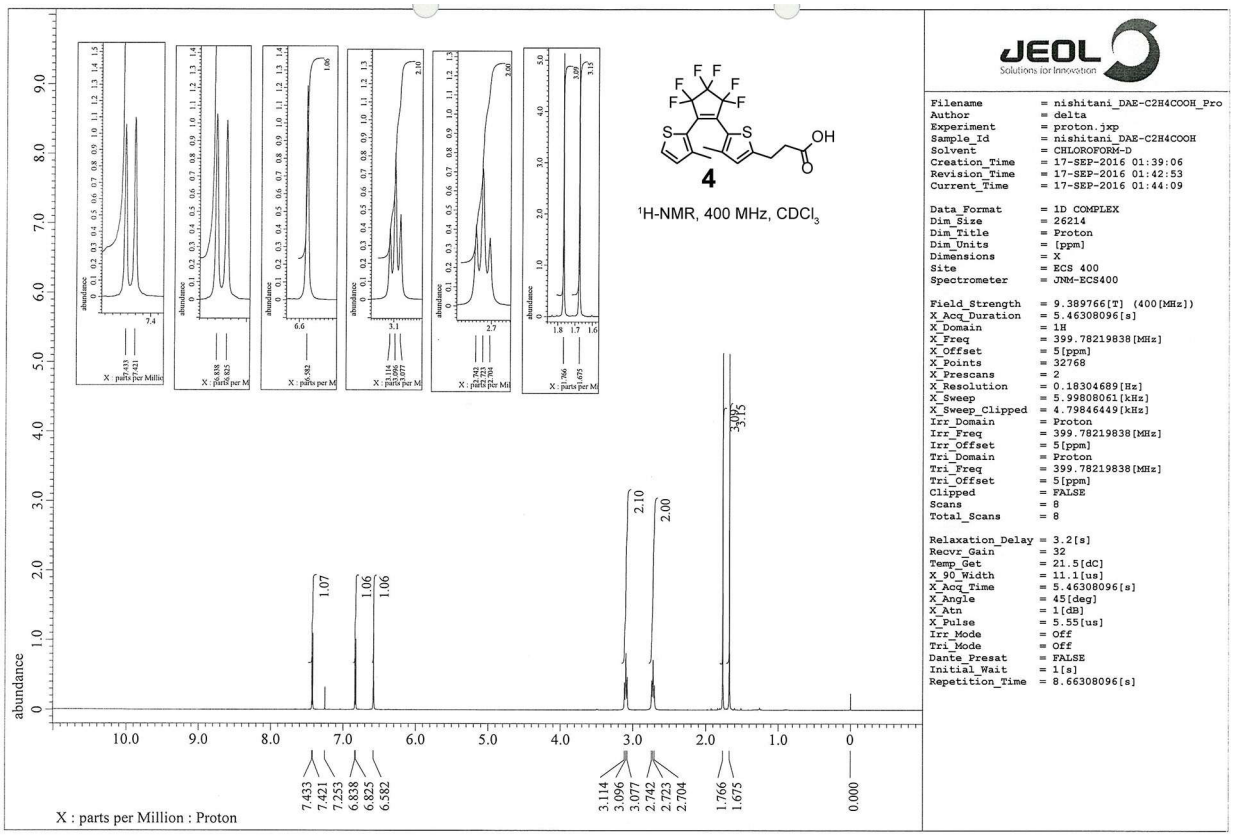

Figure S16. ^{1}H NMR spectra of compound **4** ($CDCl_3$, 400 MHz)

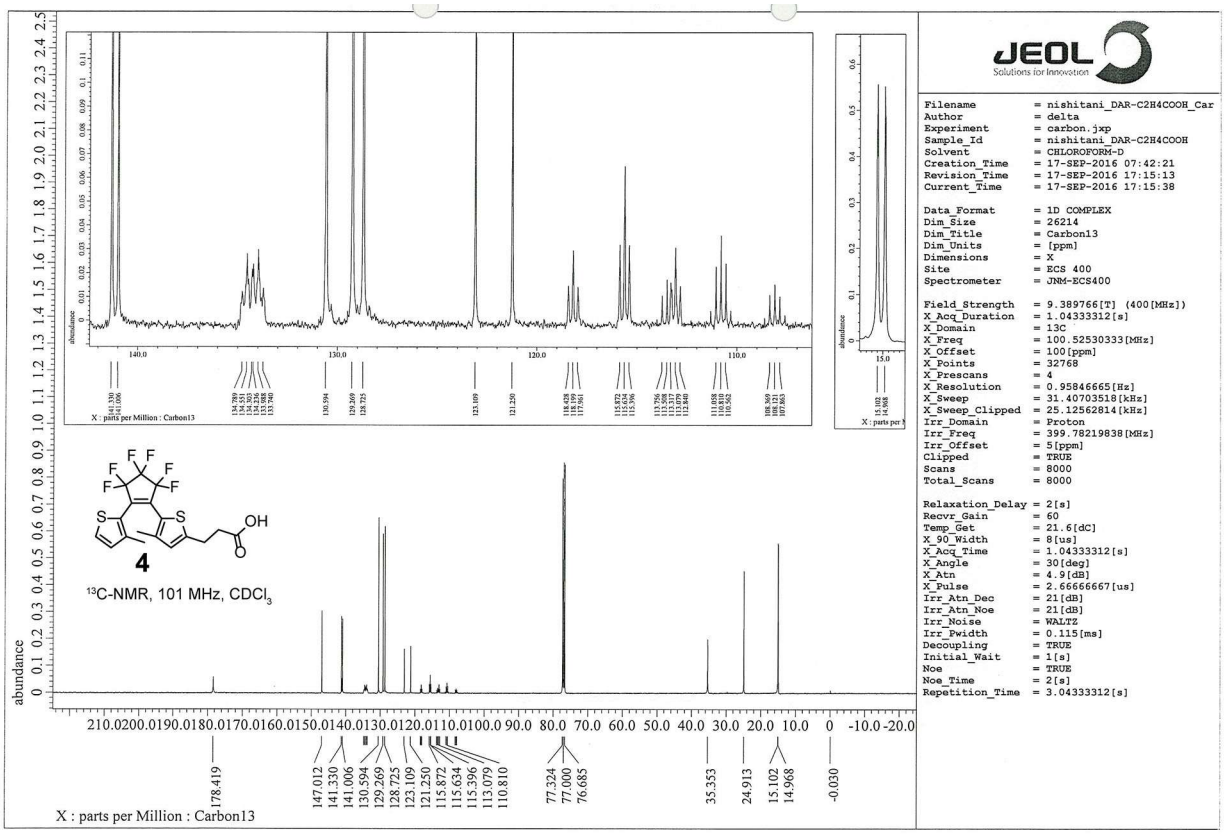

Figure S17. ^{13}C NMR spectra of compound **4** ($CDCl_3$, 101 MHz)

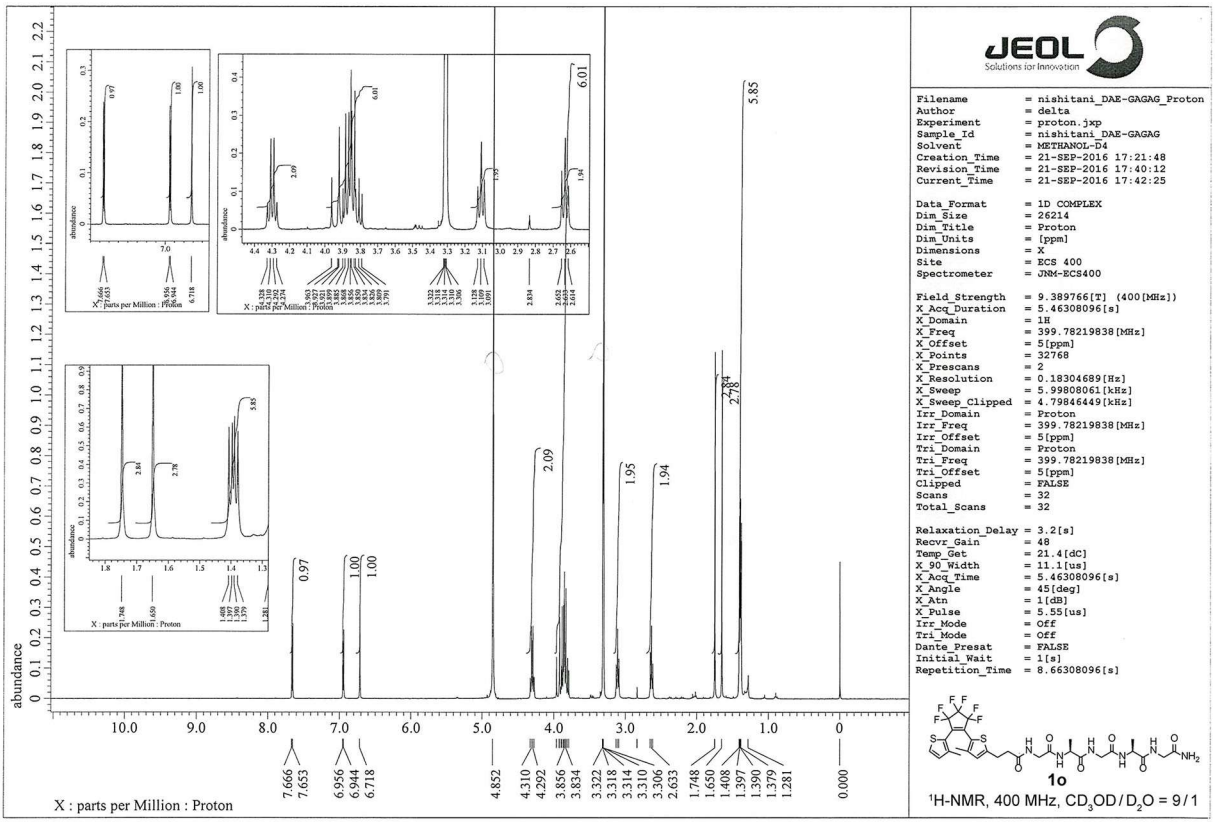

Figure S18. ^{1}H NMR spectra of compound **1o** (CD_3OD/D_2O = 9/1, 400 MHz)

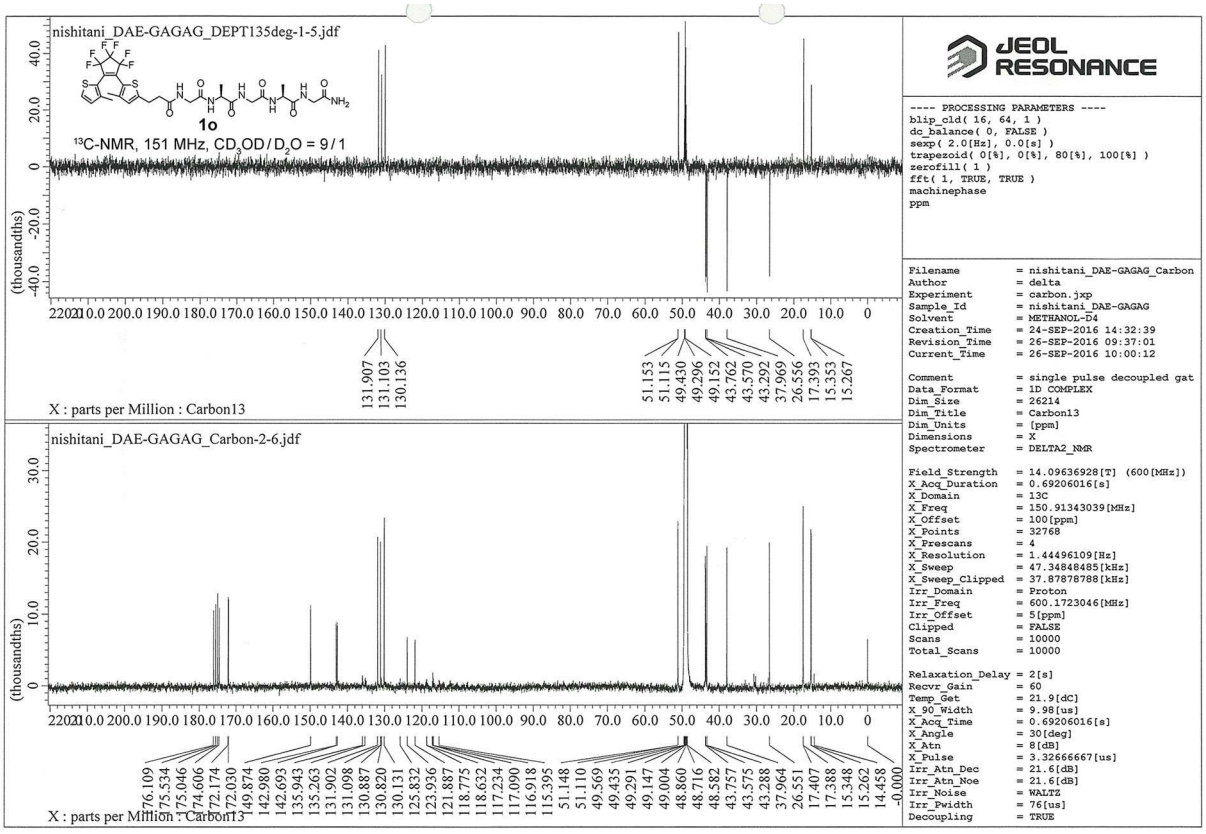

Figure S19. ^{13}C NMR spectra of compound **1o** (CD_3OD/D_2O = 9/1, 151 MHz)

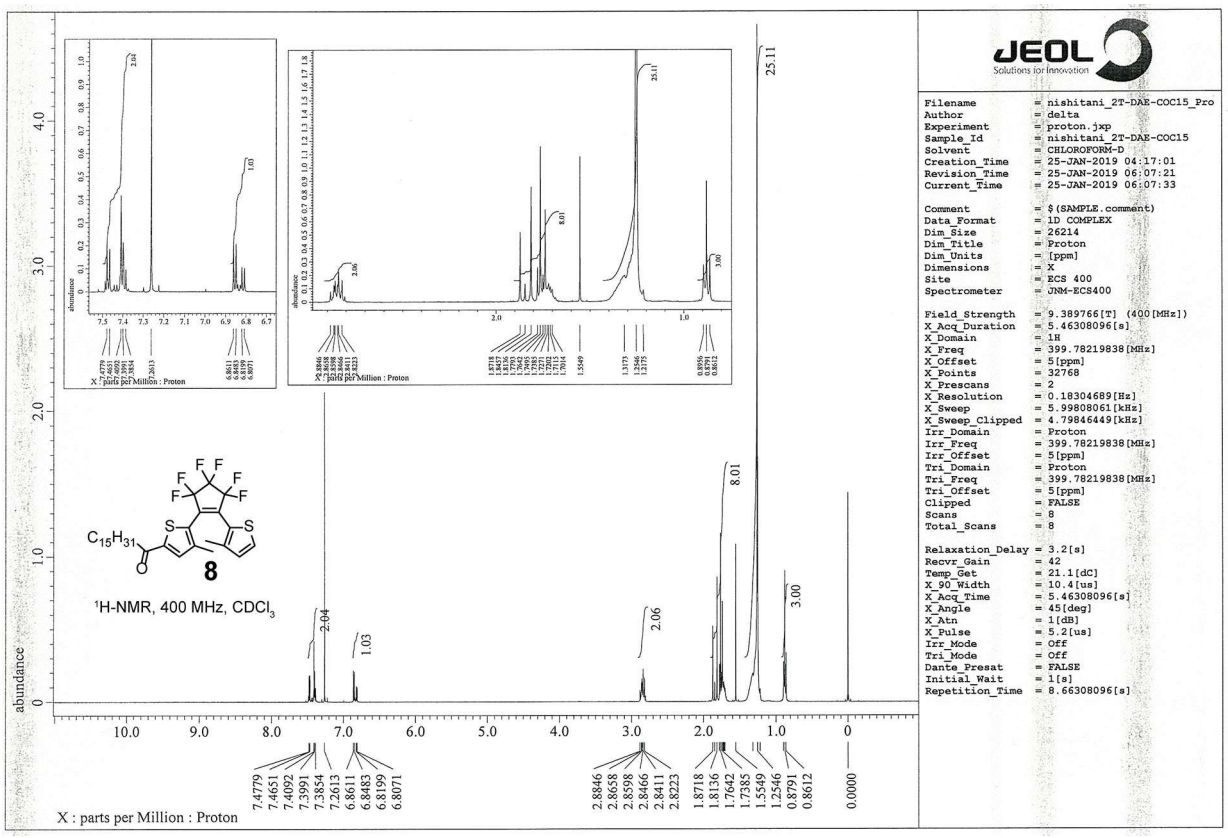

Figure S20. ^{1}H NMR spectra of compound **8** ($CDCl_3$, 400 MHz)

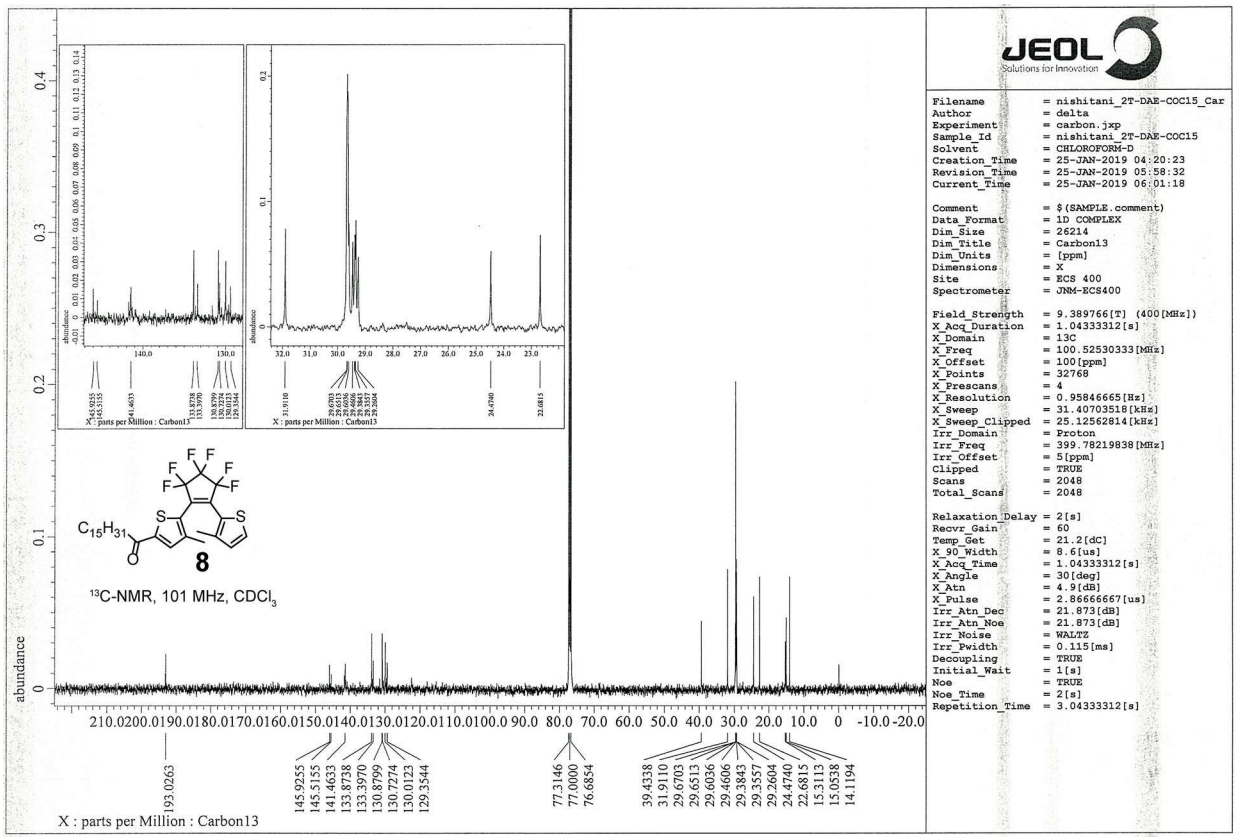

Figure S21. ^{13}C NMR spectra of compound **8** ($CDCl_3$, 101 MHz)

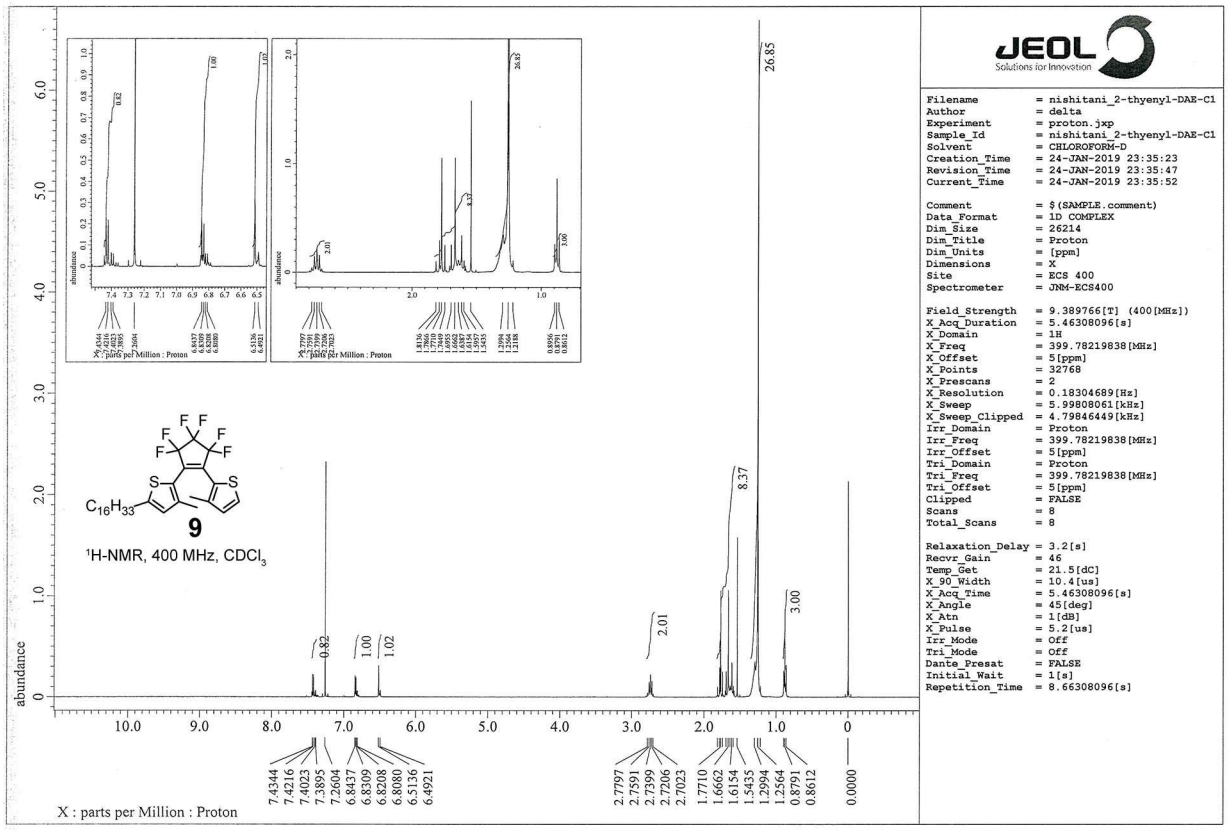

Figure S22. ^{1}H NMR spectra of compound **9** ($CDCl_3$, 400 MHz)

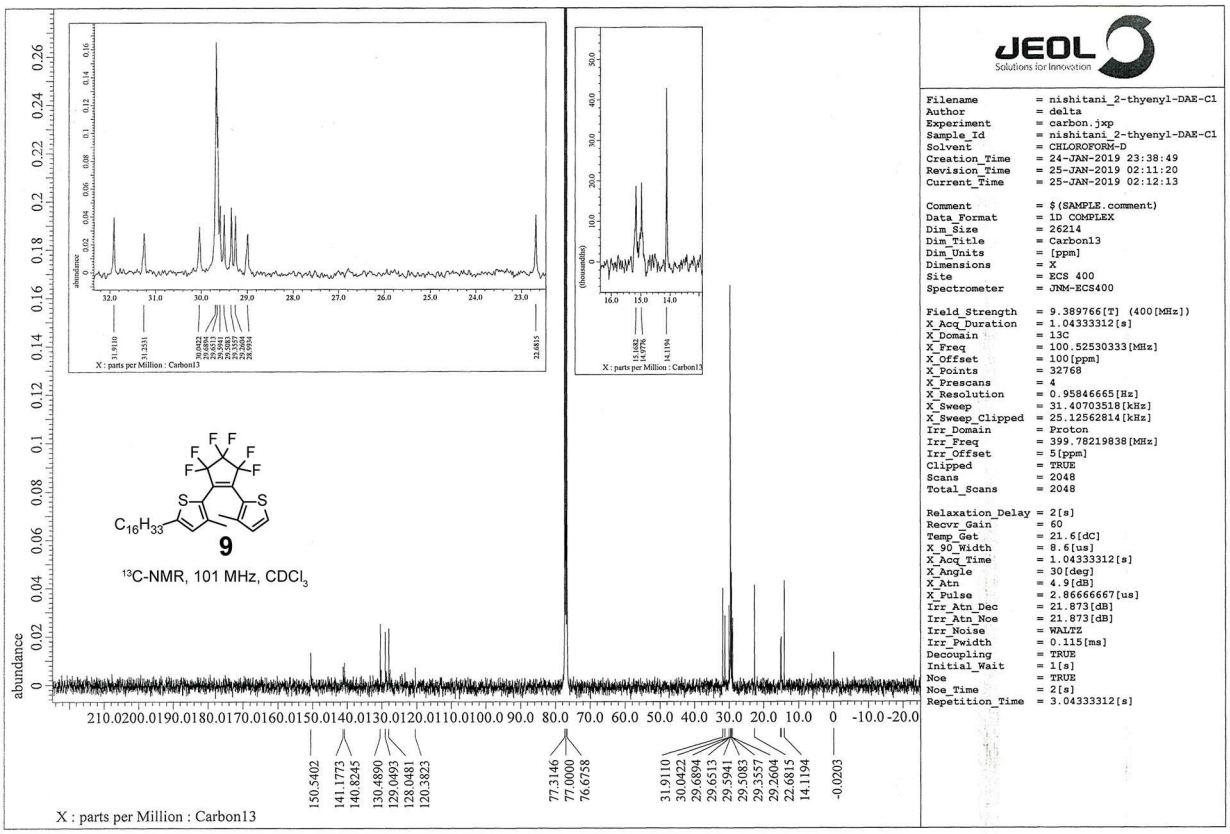

Figure S23. ^{13}C NMR spectra of compound **9** ($CDCl_3$, 101 MHz)

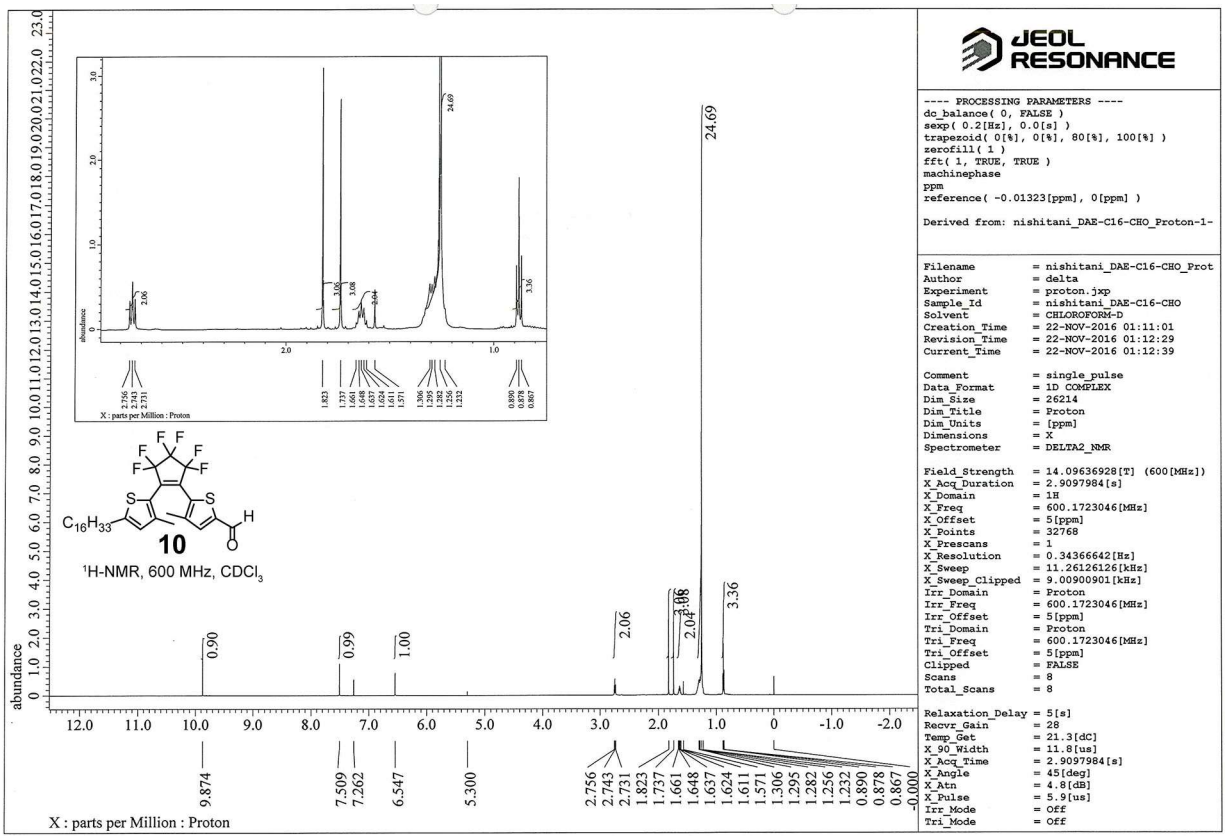

Figure S24. ^{1}H NMR spectra of compound **10** ($CDCl_3$, 600 MHz)

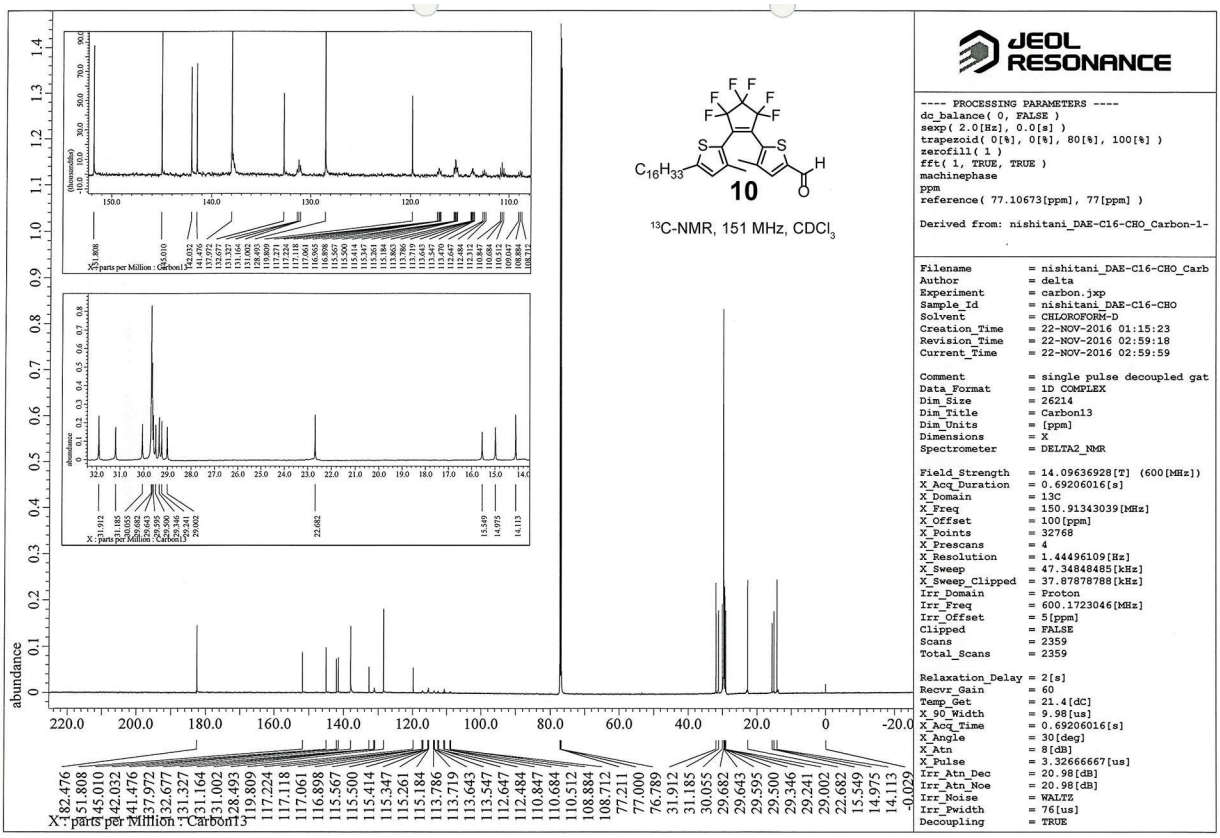

Figure S25. ^{13}C NMR spectra of compound **10** ($CDCl_3$, 151 MHz)

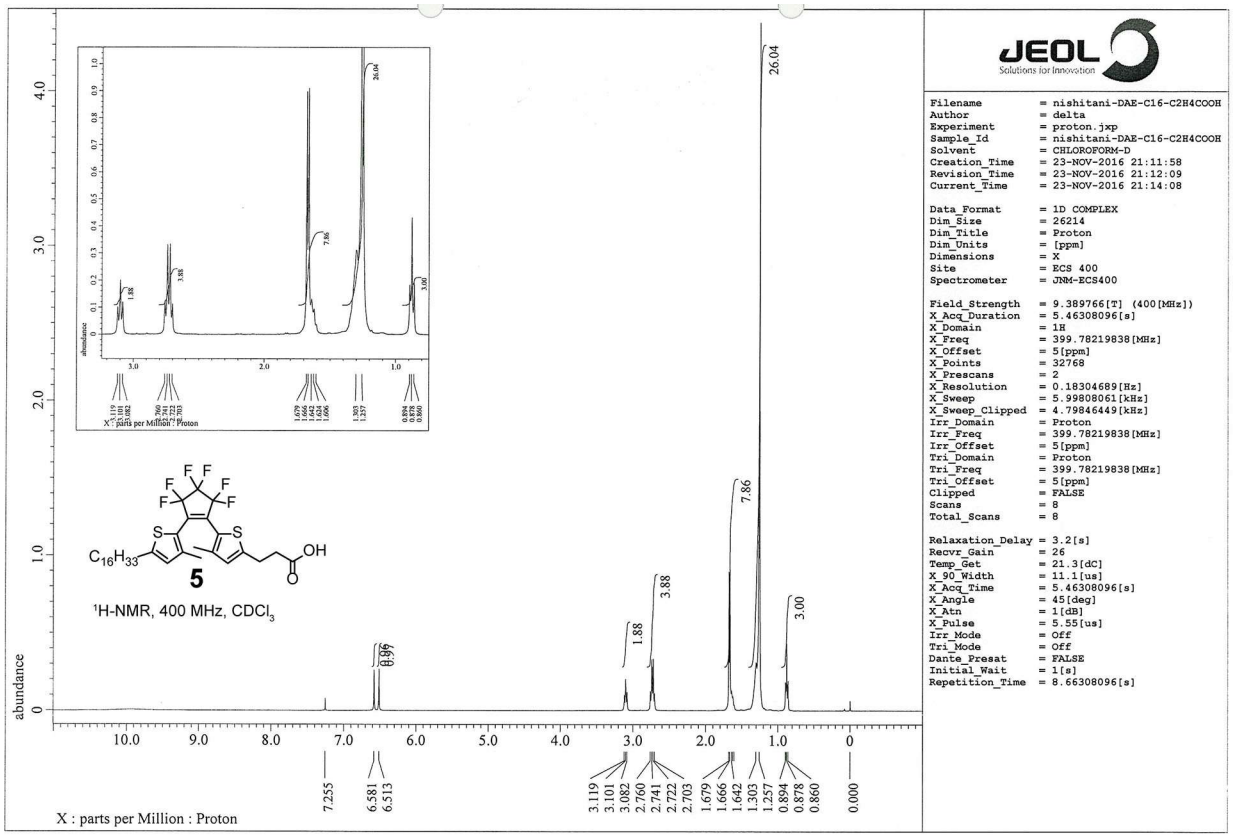

Figure S26. ^{1}H NMR spectra of compound **5** ($CDCl_3$, 400 MHz)

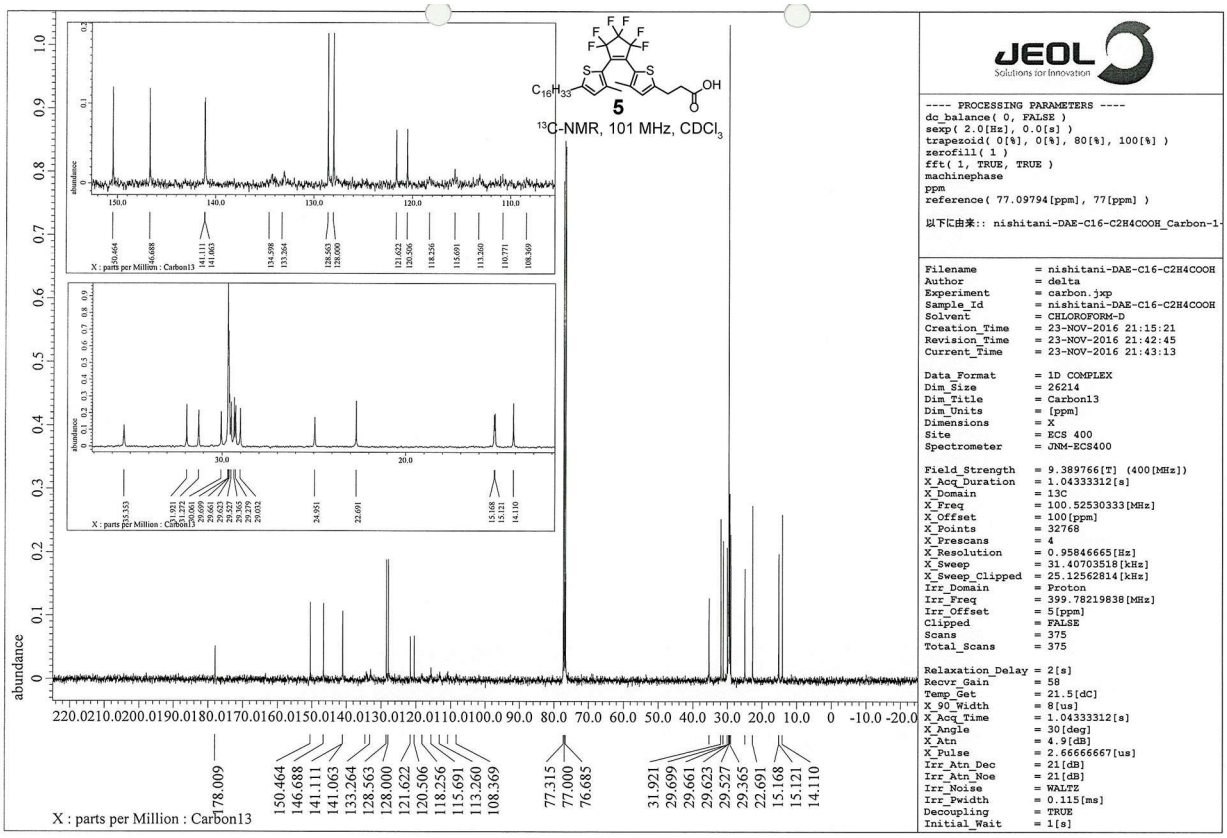

Figure S27. ^{13}C NMR spectra of compound **5** ($CDCl_3$, 101 MHz)

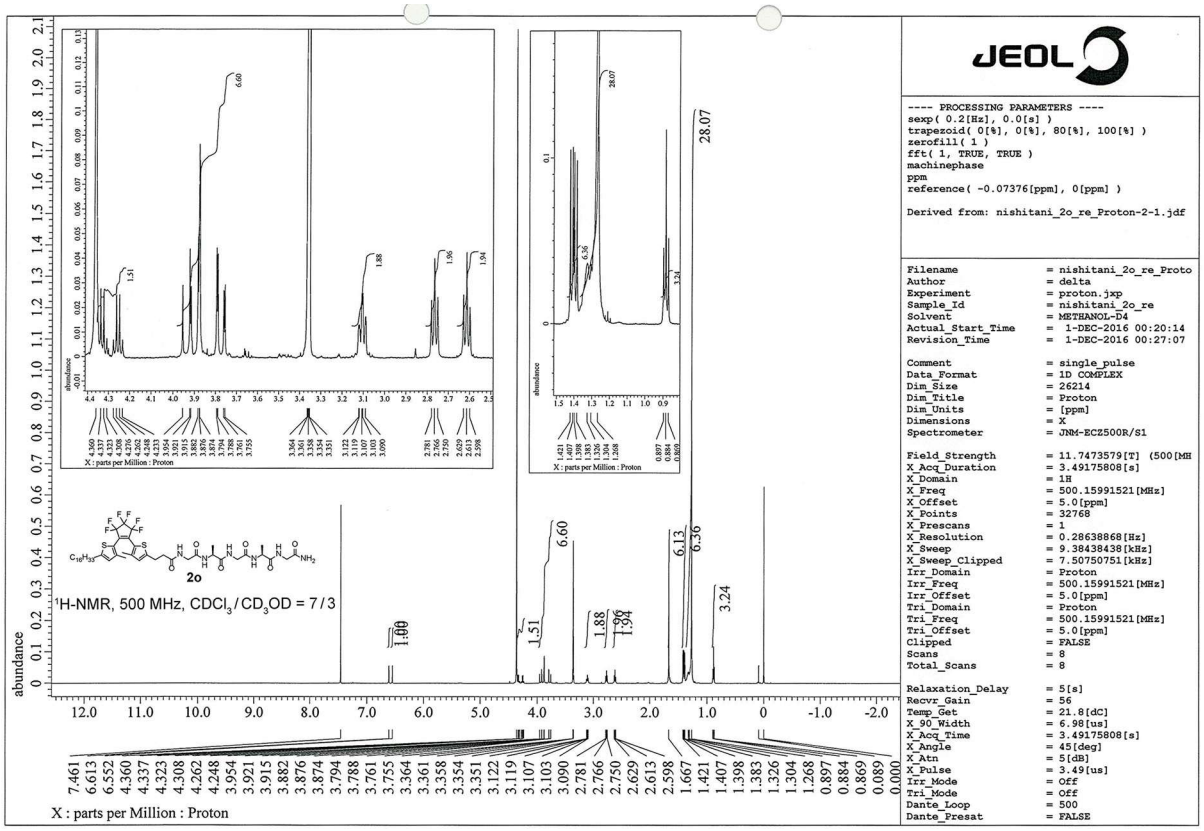

Figure S28. ^{1}H NMR spectra of compound **2o** ($CDCl_3/CD_3OD$ = 7/3, 500 MHz)

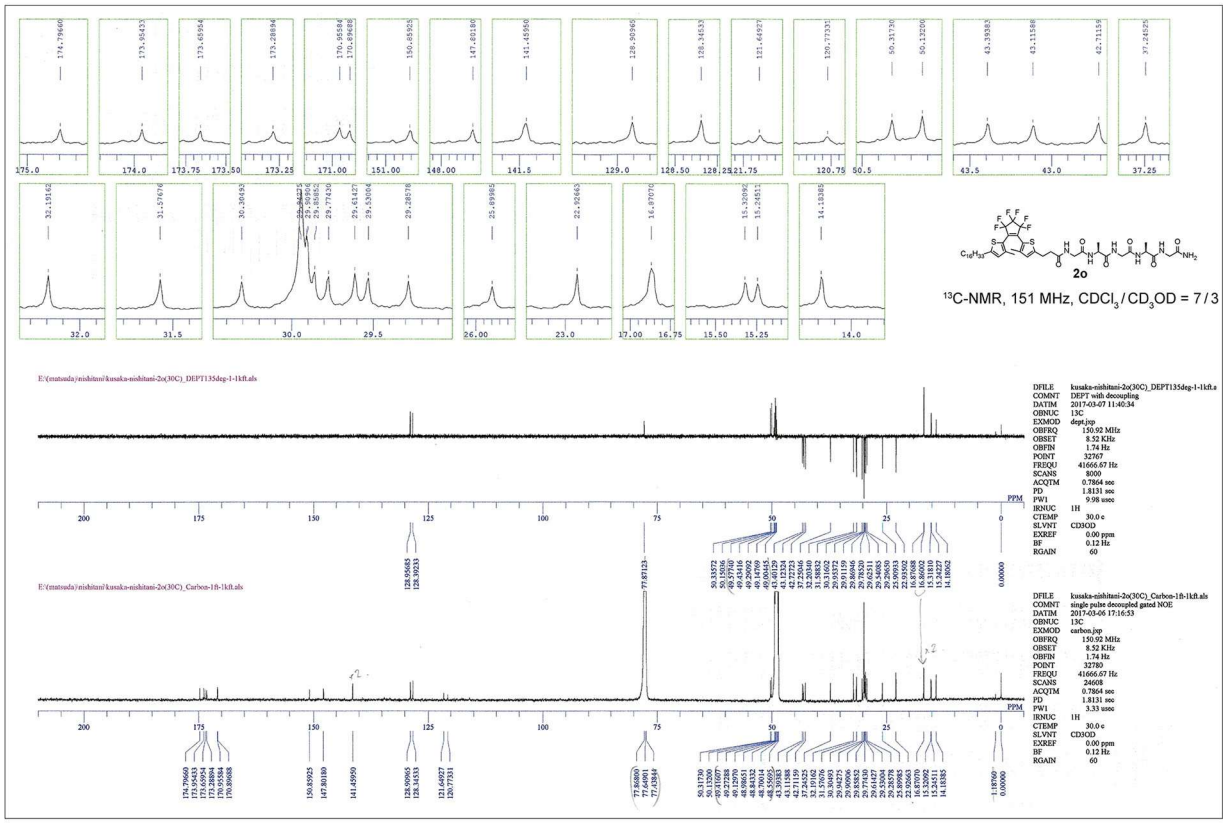

Figure S29. ^{13}C NMR spectra of compound **2o** ($CDCl_3/CD_3OD$ = 7/3, 151 MHz)

References

[S1] T. Fukaminato, T. Kawai, M. Irie, *Proc. Jpn. Acad. Ser. B* **2001**, *77*, 30–35.

[S2] S. Yokoyama, T. Hirose, K. Matsuda, *Chem. Commun.* **2014**, *50*, 5964–5966.